Towards a New Mobility Concept for Regional Trains and Hydrogen Infrastructure

F. Piraino, M. Genovese, P. Fragiacomo*

Department of Mechanical, Energy and Management Engineering, University of Calabria, Arcavacata di Rende, 87036 Cosenza, Italy

* Email: petronilla.fragiacomo@unical.it

ABSTRACT

In this paper, an integrated system, refueling infrastructure-hydrogen hybrid fuel cell train, is deeply investigated as an advanced mobility application. The proposed system is analyzed in terms of energy performance and economic aspects. Detailed numerical modeling is performed, to size and simulate the main components of the hydrogen facility and fuel cell hybrid train, on a 140-km regional line located in Southern Italy. For the hybrid railways, two 180-kW fuel cells, in parallel, are used both for passenger and freight locomotives. To size the hydrogen fueling station, 1-day operations are considered, with a hydrogen consumption of approximately 250 kg. The station resulted to be mainly composed of a 670 kW-PEM electrolyzer, producing 260 kg of daily hydrogen, stored at 350 bar. A sensitive analysis is proposed, focusing on the main system parameters, varying the passenger number and freight weight of ±20%. Promising results are reached, demonstrating the feasibility and benefits of the system, in terms of energy performance, with a fuel cell efficiency higher than 47% and a facility efficiency over 50%, maintaining high values even in the most demanding scenarios.

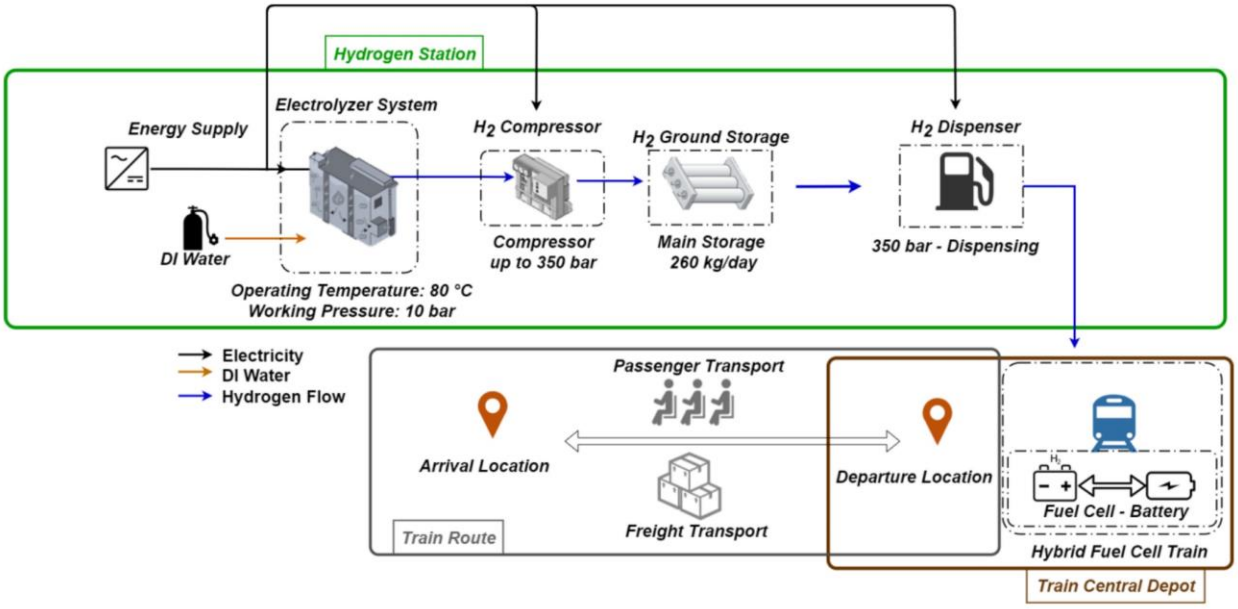
Via the financial analysis, attractive financial indicators have been reached, e.g. levelized cost of hydrogen and total cost of ownership respectively of about 8 €/kg and 12 €/km, and return on the investment of almost 19%, confirming the huge potentiality of hydrogen technology applied to heavy-duty transport.

Keywords: Hydrogen Station, Fuel Cell Hybrid Train, Passenger and Freight Transport, Advanced Mobility, Techno-economic analysis, Numerical Modeling

Highlights

- The hydrogen train shows high-energy performance and reduced hydrogen consumption
- The integrated infrastructure operates with an energy efficiency of over 50%
- Simulation of daily operation and refueling schedule
- Interesting financial results for the analyzed business case

Graphical Abstract



1. INTRODUCTION

Energy efficiency-related actions could play an important role in achieving climate mitigation goals and sustainable development targets [1]. Among the United Nations Sustainable Development Goals (SDGs), energy and climate actions are treated as key targets [2].

In particular, the SDG 13 promotes efforts toward climate actions, in accordance with the Paris Agreement. Improvements in energy efficiency and sustainable infrastructures are the core of the SDG 7, dealing with the "promotion of affordable and clean energy" (SDG 7). The SDG 9 targets aim to develop resilient infrastructures and sustainable industrialization, employing innovation. Nowadays, these actions have been also considered as potential key factors to tackle the energy issues raised during the COVID-19 emergency [3].

Considering this context, hydrogen treated as an energy vector has a tremendous potentiality in several sectors, tackling various critical energy challenges [4]. Its applications contribute to decarbonizing different sectors [5], guaranteeing an effective process with flexibility and high efficiency [6] and serving as long-term energy storage [7].

With particular reference to the mobility sector, hydrogen refueling stations are the key infrastructures related to hydrogen storage and delivery.

Apostolou and Xydis [8] offered a comprehensive literature review on the hydrogen station's actual state of the art, including future perspective and expected outcome. In their review, it is outlined the increasing trend of hydrogen station installations, identifying two main axes to be ensured: development of infrastructures to support the mobility, and increasing in the spreading of the fuel cell electric vehicles (FCEV). Research actions are indeed needed since these infrastructures still have critical points. They could be compared to industrial facilities that have to operate with aggressive conditions of pressure and temperature [9]. The refueling process itself is the most critical operation, requiring pressurized hydrogen, up to 800 bar, and low temperature, down to -40°C, to guarantee a safe and fast fill for fuel cell hydrogen vehicles. Mayyas and Mann [10] offered a deep overview of this infrastructure maturity and market readiness, focusing on their manufacturing competitiveness. As the main result of their analysis, the components related to the dispensing process (storage tanks, the balance of the plant system related to the compressors, and dispenser) resulted to be the most important contributors to a station overall cost. In this regard, niche research actions aimed to investigate the operation of hydrogen compressors [11]. Ligen et al. [12] investigated the performance of mechanical hydrogen compressors via a series of experimental activities, obtaining a comprehensive set of data identifying the performance of the compressors as a function of several operating parameters, while Genovese et al. [13] analyzed the minimum number of buffer tanks needed during a directly pressurized refueling process via booster compressors, to avoid pulsation-related phenomena.

Even these critical points, research efforts, industry interest, and governmental actions are strongly supporting the installations of hydrogen infrastructures, as outlined by Kurtz et al. [14], and the number of stations is rapidly increasing.

Safety and hydrogen-related risks are already the subject of international research, including unintended hydrogen releases during a hydrogen station operation [15], its risk assessment [16], or in alternative hydrogen production methods [17]. Ustolin et al. [18] investigated the potential loss of integrity and reliability of hydrogen infrastructures, identifying materials and hydrogen equipment as the critical topics and issues that research has to address. Kurtz et al. [19] offered a comprehensive overview of the open-to-public hydrogen stations, called retail stations, and their reliability, by analyzing around 180,000 fueling events and thousands of maintenance-related operation events. The authors identified how around 67% of the overall downtime and maintenance events are related to actions and issues related to the dispenser and the compressors. Safety issues are mostly related to the station supply chain, if hydrogen is delivered and supplied in trailers in gaseous or liquid form [20,21]. Gye et al. [22] performed a risk analysis for a hydrogen station meant to be installed in an urban area, putting in evidence how hydrogen leaks from the dispensing units and trailers are the main critical ones. A complete database with similar hydrogen associated accidents is offered by Hydrogen Tool Portal [23].

To lower safety risks, a smart option towards the hydrogen economic system transition is a hydrogen station configuration characterized by an on-site production via water electrolysis. This station layout can reduce the frequent need for external trailers, offering reliability and avoiding potential accidents in the supply chain, trailer failures, and energy inefficiencies throughout the transport.

Hydrogen station configuration with an on-site electrolysis unit could also enable a better logistic, a lower environmental impact, and a potential match with local renewable energy sources.

Concerning these topics, Gu et al. [24] performed a technical and economic assessment of several production processes and hydrogen supply pathways, by considering solar energy in different Chinese areas. Among the options, the authors considered liquid hydrogen, gas trailers, methanol as an energy carrier, and water electrolysis. All of them were compared to coal-hydrogen production in terms of economics, distance, and carbon taxes. On-site production via water electrolysis showed itself as the best option in terms of environmental impact, and also in terms of energy efficiency. Kiaee et al. [25] analyzed the performance of an existing hydrogen station in Norway, focusing on the operation of an alkaline water electrolyzer, with a working pressure of 1.2 MPa, coupled with two renewable energy power plants: wind and solar. The authors investigated the response of the electrolyzer to the supplied intermittent renewable power. Among the analyzed parameters, the stack power the gas impurities were reported, as well as the operation of the electrolyzer rectifier, providing useful guidelines for the electrolyzer technology installation and operation. Lee et al. [26] investigated the performance of a PEM electrolyzer operating at high-pressure and the potential economic benefits related to its installations. A sensitivity analysis was performed, considering variations up to ±30% of the nominal capacity, 700 m^3/hr, finding how the electricity price, the equipment cost, and the construction share the highest rate and contribution to the overall cost. Ismail et al. [27] proposed a mathematical model to analyze the combination of a solar power plant coupled with a PEM water electrolyzer. The model was implemented in Matlab, in order to directly couple the photovoltaic panels and the electrolyzer, minimizing the losses and guaranteeing a high hydrogen production. The integrated system showed a combined efficiency of almost 15%.

Based on the benefits and potentialities of this technology, several authors analyzed the research issues and the performance of different hydrogen systems and infrastructures based on the process of water electrolysis, both via numerical simulation and experimental activities, adopting different approaches.

Groppi et al. [28] performed a techno-economic assessment, flanked with an environmental analysis, of a hybrid energy system, composed also of a 90 kW electrolyzer, serving Favignana Island (Italy) in terms of transportation and energy storage. The system resulted to have important performance, in terms of economic benefits and technical operation, as well as good reliability, studied via sensitivity analysis. Mehrjerdi et al. [29] investigated the feasibility of an integrated hydrogen system for a building, aiming to achieve the performance of a "net-zero energy buildings". To face the uncertainty and the seasonality of the renewable sources often considered for these applications, the authors proposed hydrogen as the system energy storage, produced via water electrolysis in time of energy surplus, and fed to a fuel cell when power is needed. The system optimal capacity was also investigating, resulting to be about 12 kg of hydrogen, dealing with and facing the intermittency problem, and performing a reliable operation.

Xu et al. [30] proposed a novel approach to the sizing of a hybrid energy system, based on a data-driven approach via a multi-criteria and multi-objective optimization. The authors applied the approach to an energy system composed of wind turbines, solar photovoltaics, and hydrogen technologies, then validated with data coming from an existing power plant located in China. The adopted algorithm showed a system minimum levelized cost of energy and optimal energy performance with an electrolyzer size of 54 kW, a fuel cell system installed power of 20 kW, and a hydrogen storage of 450 m^3.

Bhattacharyya et al. [31] analyzed the hydrogen production process coupling alkaline water electrolysis and solar energy via photovoltaic panels. In particular, the authors estimated the solar irradiance for Mumbai, an Indian location, calculating the potential energy production and the corresponding hydrogen generation, for each day of the year and daily sunshine hours. Hydrogen production was also investigated in extreme temperature conditions, by considering the minimum and the maximum temperature values registered in the chosen site. The electrolyzer size resulted to be around 60 kW by producing 10 Nm^3/hr at 5 bar and 70 °C, and the economic analysis showed also a payback period of about 12 years. Fragiacomo and Genovese [32] proposed an innovative hydrogen infrastructure concept for hydrogen light mobility (FCEVs) and hydrogen injections in the natural gas grid. The infrastructure was investigated via numerical simulations, with an ad-hoc implemented model, with three different renewable sources: wind, solar, and geothermal energy. The energy performance of each site was investigated, and an economic and environmental analysis was performed, too, including also the benefits offered by these technologies in terms of health and quality of the air.

The presented literature review gives an exhaustive overview of how hydrogen stations are worldwide investigated by the scientific community, and they are analyzed from several and different points of view.

At the same time and with a marked pace, advanced hydrogen mobility is becoming a reality, increasing in popularity and showing high efficient performance [33], manly given by ongoing research on innovative layout and materials for proton exchange membrane fuel cells [34]. Among the several key benefits, the scientific community recognizes hydrogen technologies as virtually zero-emission vehicles [35], noiseless, more efficient than traditional

vehicles [36], and as a potential resource for the transport sector de-carbonization, above all in railway applications [37].

Fuel cell-based trains could indeed be a suitable alternative to the Diesel ones; for a specific regional line, as investigated in [38] over the British route Birmingham Moor Street to Stratford-upon-Avon and return, they can achieve an efficiency improvement of 20%, a decrease in energy demand of 55%, and a reduction in carbon emissions of approximately 70 % when compared to Diesel locomotives [38]. Besides, fuel cell technology introduction obtains positive results also in support of conventional electrified lines, as a secondary propulsion system, especially in case of electric disruption or discontinuous overhead lines [39]. In line with these topics, a detailed review is proposed by Siddiqui and Dincer [40] who have classified the main research works according to different areas, such as: prototype design/analysis, energy management, feasibility, and economic assessment and environmental performance. Among them, a particular focus is on numerical and experimental model designs and energy management systems, developed through the implementation of innovative methods and high-performing strategies.

The component selection for a specific tramway cycle is presented by in [41]; three powertrain configurations are tested (namely fuel cell-battery, fuel cell-supercapacitor, and battery supercapacitor), analyzing the vehicle performance and highlighting the satisfying fuel cell behavior, with efficiency around 49%. Not only the energy sources but also the power electronics devices play a crucial role; Fernandez el at., in their wors [42,43], a single DC/DC converter and a two DC/DC converter powertrains are tested for a fuel cell-battery tramway; suitable degrees of hybridization are evaluated and good performance is achieved for two control systems tested: state machine and cascade control strategies. Among the innovative power-sharing strategies presented, significant importance is on optimization strategies: Zhang et al. [44] proposed an equivalent consumption minimization strategy, tested on a full-size prototype, achieving satisfying experimental results, with approximately 1.5 kg H2 for a 2.4 km-journey. These strategies have a huge impact also on rail operating costs [45]: a Firefly Algorithm Optimization-Based control is numerically tested, having a daily operating cost of $304.99 per day. The whole powertrain investigation has been performed by Piraino and Fragiacomo [46], by means of a detailed energy efficiency analysis; energy sources, power electronics, and drivetrain components are numerically modeled and tested through a multi-method control strategy, reaching 42.5% overall vehicle efficiency. Among the innovative power-sharing strategies presented, significant importance is on optimization strategies: Zhang et al. [44] proposed an equivalent consumption minimization strategy, tested on a full-size prototype, achieving satisfying experimental results, with approximately 1.5 kg H2 for a 2.4 km-journey. These strategies have a huge impact also on rail operating costs [45]: a Firefly Algorithm Optimization-Based control is numerically tested, having a daily operating cost of $304.99 per day. Along with performance and economic aspects, important considerations should be carried out on safety issues. Crucial attention is focused on hydrogen system locations: Miller et al. [47] and Peng et al. [48] suggest a roof location because of harmless hydrogen dissipations, in case of a leak, and minimum damage possibilities, in the event of rail incidents. For this hydrogen system layout, 350 bar tanks, lighter than 700 bar ones, are strongly recommended in order to maintain the vehicle center of gravity in safety ranges. In addition, especially in railways, 700 bar tank use is not indispensable since different 350 bar tanks can be located on all the car roof, without incurring space issues and guaranteeing a suitable hydrogen amount for the required operations.

To support the spreading out of these innovative vehicles, hydrogen stations are needed for the exploitation and the refueling [49]. Therefore, a research question lays in the interconnection and operation of hydrogen infrastructures and advanced mobility systems. To the best knowledge of the authors, the integration of a hydrogen refueling station with hydrogen trains has not been deeply analyzed yet, as previously investigated by the authors [50]. Moreover, a better understanding and investigations of the involved energy parameters could strongly support the sustainability of these systems, by producing relevant data analysis that can enable better decisions on their operation. As a matter of fact, an energy analysis could lead to produce relevant statistics or to enable data-driven decisions. As a strong and powerful tool, modeling could help to address important global challenges dealing with climate change and clean energy solutions. The fourth industrial revolution is indeed offering a new role to numerical models and tools, which can contribute to the deployment of renewable energy and optimized energy applications and uses, leading to important cost savings.

To address this research gap, and considering also that modeling actions and in-depth assessment are beneficial to support and sustain hydrogen advanced mobility technologies in their rolling-up and execution, thanks to more comprehensive energy analysis, the activity presented in this paper aims to give its contribution to the scientific community by presenting a mathematical model and investigations on the integration of a hydrogen infrastructure connected to a fuel cell (FC) hybrid train as an advanced mobility application.

In particular, the study of the railway and the hydrogen infrastructure performance are presented, considering results achieved for passenger and freight trains that operate on a regional track. After the vehicle performance investigation, a suitable sizing for the hydrogen station is carried out. A dispensing schedule is designed in accordance with the route features and to the operation of both the trains and the hydrogen station.

The performances of the system are indeed simulated and presented for the applied case-study, which includes the estimation of the energy demand, the integration of the associated components, sensitivity analysis of the main system parameters, and a comprehensive financial assessment.

2. NUMERICAL MODELING

The present paper aims to investigate a case study concerning a regional rail line, fueled by a hydrogen infrastructure. Therefore, two different systems are taken into account, the FC hybrid vehicle and the hydrogen facility; their models are formalized and numerically implemented by means of dynamic algorithms, which are designed ad-hoc and validated with real data. The behavior of each main component is investigated in detail and modeled through thermodynamic, electrochemical, physic, and logic relations.

2.1 Model – Fuel cell hybrid train

A standard regional train with a fuel-cell based propulsion is used in the simulation. Although the main powertrain components are the core of the vehicle model, preliminary calculations are fundamental to achieve the power and energy demand of the railway for a specific line. The track morphology, drive cycle speed and vehicle features are considered the input parameters; therefore, an equation system, based on the Newton law of motion, is needed to calculate train demands. The preliminary vehicle model is based on the Equation 1, where the tractive force is achieved as the sum of three terms: the effective mass (M_{eff}) times acceleration (a); the resistive forces (F_{res}); a term that depends on the track morphology [51].

$$F_{tr} = M_{eff}\frac{dv}{dt} + F_{res} + 9.81\, M\, sin(\gamma) \quad \text{Eq. 1}$$

The resistive forces are achieved employing the Davis relation since they can be represented by means of a quadratic curve of the vehicle speed [51]. A, B and C terms depend on the vehicle characteristics: in detail, the A parameter takes into account the mechanical resistances, while the B and C terms represent the non-aerodynamic and aerodynamic drag respectively. Therefore, each parameter of Equation 2, which is useful for calculating the tractive force, depends on the train mass and, hence, passenger number and freight weight.

$$F_{res} = k_{Dav,1} + k_{Dav,2}v + k_{Dav,3}v^2 \quad \text{Eq. 2}$$

The power demand is provided by a hybrid powertrain composed of a fuel cell stack, used as the prime mover, and a battery pack, capable of providing energy and power variations [41]. Both systems are implemented by means of an equivalent circuit, composed of a controlled voltage source and a resistance [52,53]. To have a suitable computational burden with good accuracy, several simplifications have been considered, such as the gas ideal behavior and the supply manifold neglecting [52].

In the fuel cell model, the input of the controlled voltage source is the Nernst voltage, calculated as Equation 3. The equivalent resistance is variable, to achieve the real fuel cell voltage as output, considering voltage and auxiliary losses. A detailed electrochemical model, described by the authors in [52], is implemented ad hoc to calculate the fuel cell parameter value, such as pressures, exchange current, charge transfer coefficient, hydrogen consumption, and efficiency.

$$E_{FC,n} = E_{FC,0} + (T_{FC} - T_a)\frac{(\Delta G_0)}{z\, k_F} + \frac{RT_{FC}}{z\, k_F} ln\left(\frac{p_{FC,H_2}\, {p_{FC,O_2}}^{0.5}}{p_{FC,\,H_2O}}\right) \quad \text{Eq. 3}$$

Regarding the battery, the voltage source value is achieved as Equation 4, according to the battery operations, namely, charge and discharge phases. Unlike the fuel cell, the battery equivalent resistance is considered constant. All the main parameters are obtained employing the discharge characteristics, which are assumed to be the same as the ones related to the charging phase. In addition, the battery capacity does not depend on the current, and the memory and self-discharge effects are neglected [53].

$$U_B = E_{B,0} - k_{B,p}\, S_B\, I_{B,lf} - k_{B,p}\frac{Q_{B,T}}{Q_{B,T} - Q_B} Q_B + U_{B,e} exp\left(-Q_{B,e}\, Q_B\right) - R_B I_B \begin{cases} S_b = \dfrac{Q_{B,T}}{Q_{B,T} - Q_B} & W_B \geq 0 \\ S_b = \dfrac{Q_{B,T}}{\mathrm{Q_B} + 0{,}1 Q_{B,T}} & W_B < 0 \end{cases} \quad \text{Eq. 4}$$

Both the energy sources are controlled in current through DC/DC converters; a unidirectional boost converter is selected for the fuel cell system, while a bidirectional buck/boost convert is chosen for the battery, to allow charge and discharge operations. The power electronic devices connect the energy sources to the 750 V load. The power electronic devices are crucial to managing the power sources; as a matter of fact, a control strategy is implemented to perform a suitable power-sharing between the energy sources, by imposing its decision through signal for the DC/DC converter. An Equivalent consumption minimization strategy is designed to control the powertrain. The optimization algorithm calculates the fuel cell power by using the objective function shown in Equation 5, where c_{FC} and $c_{eq,B}$ (the equivalent hydrogen consumptions of fuel cell and battery respectively) are correlated through an equivalence factor (k_{ECMS}), which has crucial importance since it links the fuel cell power calculation with the battery parameters. As a matter of fact, the equivalence factor takes into account the battery SOC, allowing a suitable fuel cell output according to the energy stored in the lithium battery. It should be underlined that the fuel cell power rate is controlled by imposing a limited variation interval, below 1.5 kW/s, to avoid premature damages. Therefore, the output parameters of both energy sources are evaluated in real-time to select the fuel cell power. In the end, the battery power is achieved by performing the vehicle power equilibrium, considering the train hydrogen demand and the fuel cell power [52].

$$W_{FC} = argmin\left(c_{FC} + k_{ECMS}\, c_{B,eq}\right) \quad \text{Eq. 5}$$

Validation tests have been performed for the whole system, besides the validation of each component, comparing simulation and real data. All the individual components achieve an adequate accuracy: the proton exchange membrane fuel cell model shows an error less than 1%, compared to real components, for the efficiency, power, and voltage trends tested over all the operating range; the lithium battery model is validated by analyzing the discharge capacity at different C-rates between the model and real component over its SOC operative range, with an error less than 2%. Once the single component validation is carried out, the whole vehicle model is validated through a comparison analysis with real data, achieved for a real FC-based vehicle on a test track. Like the validation of single components, an acceptable accuracy is reached; the error made is around 2.5%, which is a satisfying value for the presented application [51,52].

2.2 Model – Hydrogen Station

The hydrogen station is considered to be mainly composed of a PEM electrolyzer, a mechanical volumetric compressor, storage tanks, and a dispenser unit.
To analyze and simulate the performance of the main components, a mathematical model has been developed.

The choice of the PEM electrolyzer technology is driven by the strong progress in the field of PEM Fuel Cell Systems [54]. In fact, even if the alkaline electrolysis is nowadays the most economically and technically mature, the PEM technology offers greater current density and quality of hydrogen [55,56].

The hydrogen station production is modeled via a multi-physics and dynamic approach [57], involving investigations on the electrolyzer stack within four main domains: electrochemical, thermodynamic, thermal, and fluid-dynamic. The most important tracked parameters are temperature and pressure levels. The subsequent fundamental assumptions were considered with reference to the modeling phase of the PEM water electrolysis system:

- The polarization curve of the electrolytic stack can operate with a variable voltage, depending on the electrolytic cell current, the electrolyzer temperature, and geometrical properties of the electrolytic cells;
- Pressure drops are not considered, as well as no high-stress operation for the electrolyzer, wherein issues consisting of cross-permeation phenomena and corrosion take region more often;
- The temperature is considered to be uniformly distributed within the electrolyzer stack (temperature gradients between the internal components of the electrolysis unit are neglected), but variable as a function of voltage, power, and external conditions;
- Each cell presents an equal thermal nature and operation;
- The stack model is based totally on cells with the equal electric behavior linked in series. Consequently, the overall stack operating voltage may be obtained, multiplying the cell voltage by considering the overall number of the electrolytic cells connected in series.

Thermal behavior is based on a lumped thermal capacitance technique, proposed in [58], neglecting the Joule effect, and by considering the external temperature set to the ambient value. Electrolyzer temperature is indeed considered as a lumped value for the whole system, and the temperature trend can be found by solving the first-order differential equation shown in Equation 6.

$$\frac{dT_{el}}{dt} + \frac{1}{R_{el,t}\, C_{el,t}} T_{el} - \left(\frac{T_a + R_{el,t}\left(\dot{Q}_{el,cool} - N_{el,cell}\left(U_{el,cell} - E_{el,tn}\right) I_{el}\right)}{C_{el,t}} \right) = 0 \qquad \text{Eq. 6}$$

Pressure levels inside the anodic and cathodic chambers are depending on the gas flows (oxygen and hydrogen).

Inside the anodic and cathodic chambers, hydrogen ideal gas law is used, while at higher pressure, for the hydrogen storage, hydrogen real gas equation has been adopted [59]. Temperature and pressure affect the electrolytic cell voltage, as shown in Equation 7: activation phenomena, ohmic resistance, and mass transfer generate certain levels of over-voltages, added to the reversible voltage, calculated at the operating electrolyzer temperature.

$$\begin{aligned} U_{el,cell} = E_{el,rev} + \frac{R\, T_{el}}{z\, k_F} \ln \frac{p_{el,H_2}\ {p_{el,O_2}}^{0.5}}{p_{el,H_2O}} + \frac{R\, T_{el}}{\alpha\, z\, k_F} \ln\left(\frac{I_{el}}{I_{el,0}}\right) \\ + \frac{t_m\, I_{el}}{A_{el}(0.005139\, \lambda_m - 0.00326)\, exp^{\left|1268\left(\frac{1}{303} - \frac{1}{T_{el}}\right)\right|}} + \frac{R\, T_{el}}{\beta\, z\, k_F} \ln\left(1 + \frac{I_{el}}{I_{el,lim}}\right) \end{aligned} \qquad \text{Eq. 7}$$

The electrolyzer stack power is indeed dependent on the operating current, the cell voltage, and the number of cells, as shown in Equation 8, experimentally validated in the authors' previous work [57]. The electrolyzer operates according to the hydrogen station needs: if the hydrogen production is needed, the electrolyzer will work at full power, otherwise it operates in standby mode, with a power consumption considered as a certain percentage of the electrolyzer nominal power, set to 10%.

$$W_{el,stack} = \begin{cases} N_{el,cell}\, U_{el,cell}\, I_{el} & \dot{m}_{el,H_{2,p}} > 0 \\ \%_{nom}\, W_{el,nom} & \dot{m}_{el,H_2,p} = 0 \end{cases} \qquad \text{Eq. 8}$$

The set-points chosen for the hydrogen production starting conditions are based on the hydrogen storage tank pressure levels. In particular, if the tanks are already full (e.g. they have reached the maximum pressure levels), the production stops, as shown in Equation 9. When the tanks need to be filled, the hydrogen production is mainly as a function of the operating current with a third-degree polynomial expression (deriving from the application of the Faraday efficiency) and the number of cells.

$$\dot{m}_{el,H_{2,p}} = \begin{cases} \dfrac{N_{el,cell}\, I_{el}(\, k_0 + \, k_1\, I_{el} + \, k_2\, I_{el}^2 + \, k_3\, I_{el}^3)\, MW_{H_2}}{z\, F} & p_{tank,i} < \, p_{tank,max} \\ 0 & p_{tank,i} = \, p_{tank,max} \end{cases} \qquad \text{Eq. 9}$$

The ancillary power needed for the electrolyzer auxiliary equipment is modeled with a semi-empirical trend, as a decreasing exponential function of electrolyzer stack power, shown in Equation 10.

$$W_{el,anc} = k_{anc}\, W_{el,stack}{}^{-b} \quad \text{Eq. 10}$$

The electrolyzer model has been already validated [57], showing a good match with the experimental data. As an instance, the electrolyzer power consumption (Equation 8) has shown a root-mean-square error (RMSE) value of 0.0744 kW and an RMSE Percentage (RMSEP) of 0.0159 in the range between 18 A and 135 A, and the hydrogen production flow rate (Equation 9) an RMSE of about 0.022 Nm^3/h and an RMSEP of about 0.1372 in the same range. Similar results have been obtained for the ancillary power consumption (Equation 10), polarization curve (Equation 6), voltage efficiency, and system efficiency, in the same operating range.

Besides the electrolyzer unit, the other main important energy demand belongs to the hydrogen compressor. The compression process has been simulated by considering a dynamic process via a polytropic transformation [60], with a double stage. The amount of work for each stage is expressed in Equation 11, as a function of the compressor mass flow rate, the inlet temperature (considered the hydrogen gas temperature coming from the electrolyzer), and the pressure ratio between the considered stage compressor inlet and the stage pressure outlet.

$$W_{el,c} = \dot{m}_{el,H_{2,c}} \frac{R_g\, T_{el}}{\eta_m} \left[\left(\frac{p_{c,out}}{p_{c,in}} \right)^{\frac{m-1}{m}} - 1 \right] \quad \text{Eq. 11}$$

At the first stage, the compressor inlet is considered to have the same pressure as the electrolyzer cathodic chamber, while the pressure outlet is derived from the double stage optimization [61]. The hydrogen compressor mass flow rate is thus dependent on the hydrogen cathodic chamber pressure, as shown in Equation 12. If the cathode pressure is lower than the operating working pressure of the electrolytic unit, the chamber needs to be pressurized and the compressor is considered to be shut down. When the electrolyzer is indeed operating at the nominal pressure, the compressor starts its operation, and its mass flow rate is as a linear function of the compressor pressure inlet, validated with data retrieved from a real compressor flowchart [62].

$$\dot{m}_{H_{2,c}} = \begin{cases} \left[k_{c,1} + k_{c,2} \frac{p_{el,in,H_2}}{10^5} \right] \frac{MW_{H_2}}{22.4 * 3600} & p_{el,in,H_2} \geq p_{el,target} \\ 0 & p_{el,in,H_2} < p_{el,target} \end{cases} \quad \text{Eq. 12}$$

An intercooler is also taken into account between the two compressor stages, with a coefficient of performance, CoP, equal to 1.5. The second stage of the hydrogen compressor delivers hydrogen to the storage tanks. Their operation and pressure have been modeled employing the mass conservation law and a previously proposed switching procedure [63]. For the dispensing line, the refueling process adds an overall value of 1.6 kWh/kg [64,65], with the assumption of no pre-cooling required for the 350 bar fill [66].

The discharging procedure is controlled with the intention to decrease energy consumption. The refueling process is frequently associated with an instantaneous refueling by operating the piston compressors. The energy demand of these components depends on the ratio between the pressure inside the storage tanks and the pressure inside the vehicle tank. As investigated by [62], consolidating the suction pressure can lessen power consumption. For these reasons, the storage discharging process has been assigned to the tank that, in the considered instant of time, has the very highest level of pressure.

2.3 Economic analysis

The economic investigation is based on two different analyses: a static analysis, via the application of the Levelized Cost of Hydrogen (LCOH) and Total Cost of Ownership (TCO) methods, and dynamic analysis, via the investigation of the pay-back period (PBP), the return-on-investment (ROI), and the net present value (NPV).

The static analysis aims to analyze the current technology costs with other studies and reports of the scientific literature, assessing the feasibility of the business case also in comparison with other technologies. The dynamic analysis will assess the economic benefits and the financial indicators over the whole lifetime of the proposed energy system.

For both analyses, the capital expenditure (CAPEX), operational expenditures (OPEX), and each component lifetime are needed. They have been retrieved from the most recent literature and state-of-the-art analysis and reported in Table 1. Each component cost is a function of a specific parameter: the electrolyzer system is dependent on the installed electric size, as well as the storage compressor. The water purification system is a function of the processed water flow rate, while the hydrogen storage depends on the daily storage capacity.

Table 1 – Capital Expenditure, Operational Expenditure and Lifetime for each component of the Energy System

Equipment	CAPEX [k€]	OPEX [%]	Lifetime [yr]
PEM Electrolyzer [67]	1.2/kW	4 % of CAPEX	20
WPS	1.2/m^3/day	1% of CAPEX	20
H_2 Storage Compressor [68]	$40.035 \cdot kW^{0.6038}$	2% of CAPEX	15
H_2 Storage Bank [69]	470 /kg H_2	8% of CAPEX	30
Dispensing Unit Dispenser [70]	91.810/unit	1.1% of CAPEX	10
Fuel Cell Hybrid Train [71]	5000	0.72 c€/km	15

Besides CAPEX and OPEX considered in Table 1 above, other costs have been considered. The costs for civil works will account for an overall cost of 80 k€, and the station operation will also need several permits, accounting for 15 k€. The hydrogen train, according to Roland Berger and Fuel Cell and Hydrogen Joint Undertaking Report [71], needs four operators for its operation, with an average labor cost of 32 k€ per year per each operator.

Among other operational costs, water purchase and energy supply need to be taken into account. Regarding the water purchase and supply, costs have been set according to the tariffs belonging to an Italian Water Management Company[72]. For the electricity costs, the electrical energy has been considered to be supplied by the national grid, in accordance with the Italian market scenario in terms of fees and tariffs, with reference to 2019 [73,74], by including also the costs for distribution and transmission [75].

The LCOH method [76] has been applied to set a profitable price for the produced hydrogen. As shown in Equation 13, it is calculated as the sum of the station CAPEX, scaled, and annualized through the Capital Recovery Factor, the station OPEX, and the component replacement costs. The overall values are then divided by the annual hydrogen production. CRF is considered as a function of the discount rate i and the entire life of the system n, and it is calculated utilizing the expression presented in Equation 14.

$$LCOH = \frac{C_{capex}\,\mathrm{CFR} + C_{opex} + C_{rep}}{AP_{H_2}} \qquad \text{Eq. 13}$$

$$CRF = \frac{i \cdot (1+i)^n}{(1+i)^n - 1} \qquad \text{Eq. 14}$$

Considering a system overall lifetime of 15 years, the replacement costs are mainly related to the electrolyzer stack, with an overall lifetime of 40,000 hours (replacement every 5 years), with a specific cost of 525 €/kW of installed power. Equation 15 shows the replacement cost calculation, as a function of the electrolyzer stack, the years of replacement r_j, and the cost of each replacement. Besides the electrolyzer stack replacement, after 10 years, the dispenser unit is considered to be fully replaced.

$$C_{rep} = CRF \sum_{j=1}^{q} \frac{C_{stack}}{(1+i)^{r_j}} \quad \text{Eq. 15}$$

The total cost of ownership (TCO) [77,78] is applied to compare the ownership of the integrated system (infrastructure and vehicle), with conventional technologies. It is calculated according to Equation 16. The TCO corresponds to the sum of annualized CAPEX, the yearly depreciation D, the labor cost C_{labor} (4 operators with an average yearly salary of 32 k€), the fuel cost C_{fuel} (value set after the LCOH analysis), the annual operational expenditures, subtracted by the reselling price, RP (for the purposes of this paper considered to be zero), and divided by the annual total distance driven by the hybrid fuel cell trains, TD, expressed in km.

$$TCO = \frac{C_{capex} \cdot \mathrm{CFR} - \mathrm{RP} + \mathrm{D} + C_{opex} + C_{fuel} + C_{labor}}{TD} \quad \text{Eq. 16}$$

After the static economic analysis, the key financial indicators, that have been chosen to investigate the business case via the dynamic economic assessment, are the Return on Investment (ROI), the Net Present Value (NPV), and the Pay-Back Period Analysis (PBP). To determine the NPV level, Equation 17 has been applied, calculating the discounted cash flows of the considered case study, CF_x, defined as revenues minus costs (discounted and calculated also by including the inflation rate, g), and the initial investments, considered as the sum of all the CAPEX.

$$NPV = -C_{capex} + \sum_{x=1}^{n} \frac{CF_x \cdot (1+g)^x}{(1+i)^x} \quad \text{Eq. 17}$$

The PBP is defined as the time, in years, when the NPV level is zeroed. The ROI value is calculated according to the expression presented in Equation 18, and it corresponds to the business beneficial return when compared to the initial CAPEX. D_k represents the depreciation per year, considering the contributing rate of all the components involved in the facility, calculated with fixed yearly rates for the corresponding lifespan of each component.

$$ROI = \frac{\left[\frac{1}{n} \sum_{x=1}^{n} (CF_x - D_x)\right]}{C_{capex}} \quad \text{Eq. 18}$$

3. CASE STUDY SIMULATION AND RESULTS

The investigated case study, presented in Figure 1, is composed of hydrogen production and dispensing facility, assumed to be located in a central depot, in Lamezia Terme (Italy), fueling hybrid fuel cell trains for passengers and freight transportation.

Lamezia Terme is one of the major cities located in Calabria, South Italy, offering multi-services for transportation. The city presents the main railway station of the territory, serving as central infrastructure the two Calabrian Coasts, and the main airport of Calabria. For this reason, the hydrogen production facility is considered to be located in Lamezia Terme, where electrolytic hydrogen is produced via a PEM electrolyzer, requiring deionized water (DI) and electricity, and operating at 80 °C and 10 bar of working pressure. Once hydrogen is produced, it is processed by a mechanical volumetric compressor, up to a pressure of 350 bar. Then hydrogen is stored in a main ground storage system, and from there it can be drawn to refuel the hybrid fuel cell trains.

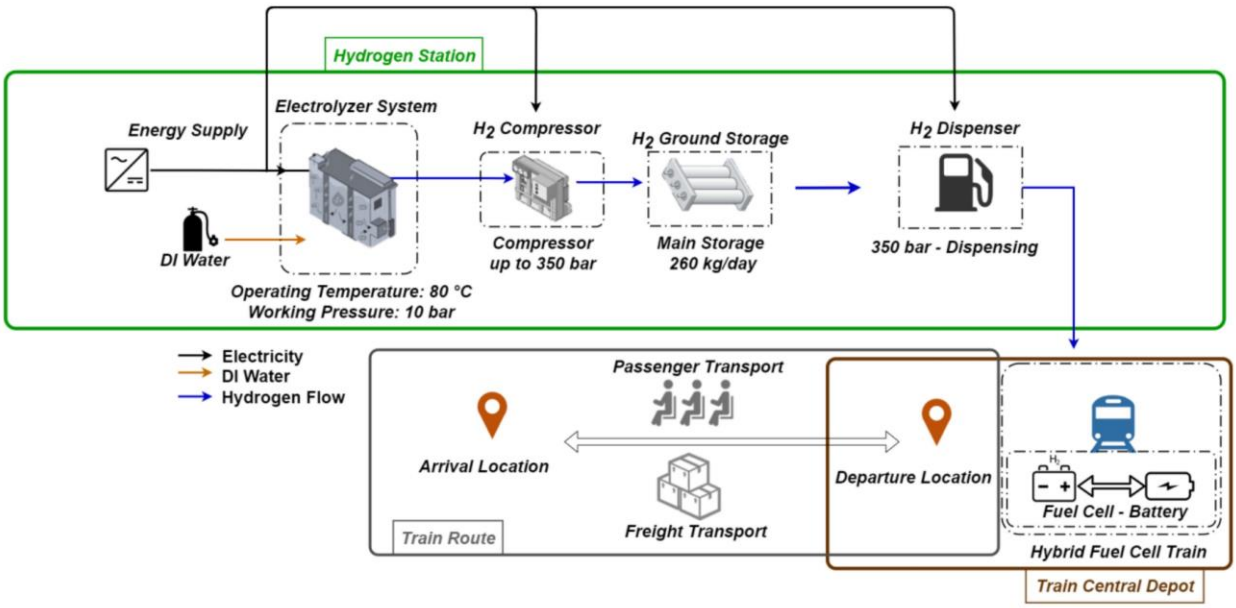


Figure 1 – Case Study Description

The two fuel cell hybrid trains have been sized and designed to transport passengers and freight from Lamezia Terme, as a departure location. The arrival location is considered to be Cosenza, since it is characterized by the presence of the University of Calabria with several students coming from different locations, and by the presence of industrial areas, needing freight transport service. Passenger and freight trains are simulated on the Lamezia-Cosenza track, which is an existing electrified line. It is a crucial track that links Lamezia, where the main Airport of Calabria is located, with Cosenza, one of the most important cities in the region.

This track is almost 140 km in length, and it can be broadly divided into two sections: the first one, from Lamezia to Paola, is part of the South Tyrrhenian line and, hence, it is along the coastline, with altitude and slope in a moderate interval. The second part links Paola to Cosenza and it mainly goes through a tunnel, because of the marked altitude difference between the two cities; as a matter of fact, the altitude and the slope vary in a greater range compared to the first line section.

Regarding the drive cycle, two different trends are considered for passenger and freight trains. The passenger drive cycle is roughly 2 hours, and 4 stops are considered for each way, with a 1-minute time stop. A simplified trend is considered and the train reaches a maximum speed of approximately 130 km/h. The freight trains drive cycle does not have intermediate stops, but it links Lamezia Station directly to the industrial area of Cosenza. They spend almost 3 hours for a round trip, reaching 80 km/h of maximum speed; in summary, the freight train speed and acceleration have lower values compared to those of the passenger vehicle.

Standard vehicles are simulated for each scenario; a two-car unit passenger train is considered, with 50 m in length and an unladen weight of almost 70 tons; it can transport a maximum of 130 passengers. With reference to the data of train passengers in Calabria [79], 100 passengers are considered for the first case per each trip. The freight vehicle is built for transporting standard good mass, with 12 wagons and an unladen weight of 300 tons; for the studied case, 200 tons of goods are considered.

According to the power and energy demands for both drive-cycle typologies, a suitable sizing test is performed as shown in Table 2 [80]. The control system manages the fuel cell to provide the total energy demand; therefore, a fuel cell system composed of two 180 kW FC stacks connected in parallel is used. The energy and power variations are provided by a pack composed of 38 Ah Lithium Iron Phosphate (LFP) batteries and two configurations are used: 100 series x 30 parallel LFP batteries for passenger trains and 100 series x 50 parallel batteries for freight transport.

Figure 2 and Table 2 show the results achieved for the passenger and freight vehicle simulations. Regarding the passenger case, the control system imposes a quasi-constant power trend (green line) to the fuel cell system; it is used to provide the whole energy demand with slow power variations, in an interval between 140 kW and 250 kW. On the

contrary, the battery pack supplies energy and power variations, and, at the end of the cycle, its energy provided is 0 kWh, since the same SOC of the initial cycle time is achieved. Therefore, the battery power output (red line) has sudden power variations, both in the negative and positive sector, within -500 kW and 600 kW, in order to respond to the vehicle demands, mainly due to track altitude and vehicle speed variations. Other crucial output vehicle parameters are listed in Table 2. The fuel cell system consumes 29.1 kg/cycle of hydrogen, with 50% average efficiency; the battery works in an appropriate operative range since both SOC and C-rate assume suitable values.

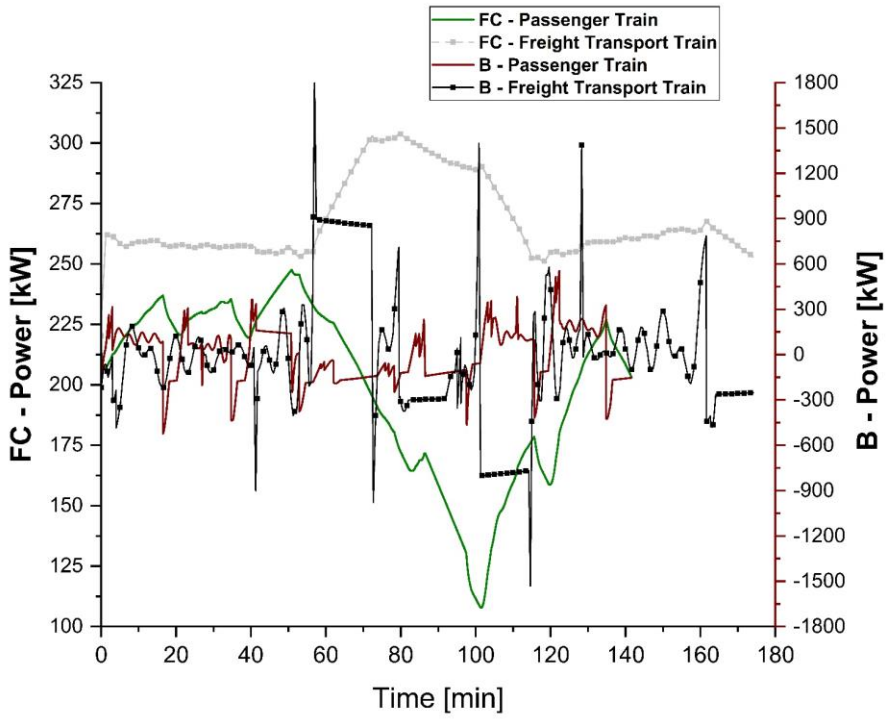


Figure 2 – Hydrogen Fuel Cell and Battery Power Request during the investigated drive-cycle

Table 2 – Hybrid Fuel Cell Trains Main Results

Train	Parameters	Value
Passenger Train	Fuel cells stack	2
	Battery module	100 S x 30 P
	Average FC efficiency	50 %
	H_2 consumption	29 kg/cycle
	Battery state of charge	[55%, 85%]
	Battery C-rate	[-1.5 C, 1.5 C]
Freight Transportation Train	Fuel cells stack	2
	Battery module	100 S x 50 P
	Average FC efficiency	48 %
	H_2 consumption	52 kg/cycle
	Battery state of charge	[35%, 80%]
	Battery C-rate	[- 2 C, 3 C]

The simulation results achieved for goods transportation are also summarized in Figure 2 and Table 2; in this case, the fuel cell and battery play the same role compared to the passenger transport train, as energy provider and power variation supplier respectively. The fuel cell power (grey line) assumes higher values compared to the passenger's case, within a narrow interval between 200 kW and 350 kW, and, therefore, a higher energy consumption. As a matter of fact, 52 kg/cycle of hydrogen are needed and, because of the high operative rate, the fuel cell has an average efficiency of approximately 47%, lower than the passenger vehicle. Regarding the battery, like the passenger railway, it provides sudden power variations (black line), in a wide interval between -1.5 MW and 2 MW, since the power vehicle demand, calculated by means of the Newton law of motion, has quite rapid power changes. The battery SOC and the C-rate vary in higher ranges compared to the previous application, respecting, however, the safety limits imposed by the Producers.

To perform the hydrogen fueling sizing, 1-day operations are considered. For passengers, 5 daily trips are scheduled, while 2 complete journeys are taken into account for goods transportation; for this reason, according to the passenger and freight weight esteemed, 248 kg of hydrogen per day are needed.

The analysis discussed is valid for a standard operating day; to make generalizations, a sensitive study is carried out, ranging the passenger number and freight weight of ±20%. Equation 1 above highlights the relation between the tractive force and the mass transported; therefore, when the mass increases, the power demand raises, along with the hydrogen consumption, and vice versa. Figure 3 below shows the sensitive analysis of the hydrogen consumption per day; the passenger and freight trains spend 243.5 kg of hydrogen for 80 passengers and 160 tons of goods and 252 kg of hydrogen for 120 passengers and 240 tons of goods. The passenger rate variation provokes a lower increase compared to the freight one, given by the amount of mass related.

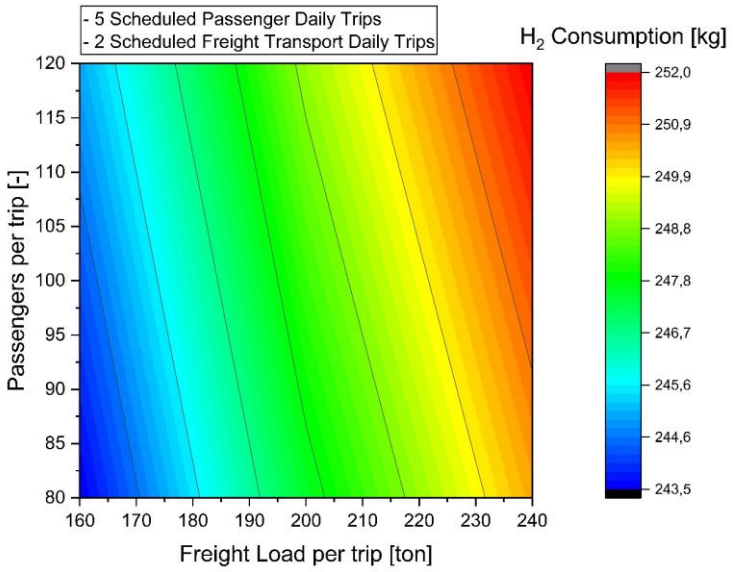


Figure 3 – Hydrogen Demand under Different Transportation Scenarios

The hydrogen station has been sized according to the most demanding daily scenario. As shown in Figure 3, with a freight load per trip of 240 tons, 120 passengers per trip and 7 scheduled routes (two for freight transport and five for passengers), the daily hydrogen request for the operation of the train resulted in 252 kg. According to a previous study, a daily operation for the hydrogen station can account for 2-10% of potential hydrogen losses [81]. Considering also these potential losses, the hydrogen production target for the station sizing has been considered 260 kg/day.

The infrastructure model input parameters are listed in Table 3, for the three main subsystems: electrolyzer, compressor, and storage tanks. The electrolyzer geometrical properties, such as the cell active area, come from the regression technique adopted during the model experimental validation, performed in the authors' previous work [57]. During the validation analysis [57], the best operating point that allows a higher efficiency was found to be around 135 A, then chosen as an input parameter for the simulation of the present case study. The number of cells has been

then scaled up to meet the required hydrogen daily production. Pressure and temperature have been chosen according to the normal operating range of this electrolyzer technology [55]. For the thermal parameters, namely the specific thermal capacity and the thermal resistance, during the model validation [57], it was previously deemed appropriate to extrapolate their values from experimental data coming from different applications in literature [54,58,82–87]. The values are presented in Table 3.

As described in the modeling section, the hydrogen compressor is modeled with affordable accuracy by assuming that the process could be described as a polytropic compression. The value of the polytropic coefficient has been extrapolated from operating hydrogen station modeling and validation [88–90]. A compressor characterization has been performed by interpolating Equation 9 with the flow chart of a commercial hydrogen compressor [62], and whose resulting values are shown in Table 3. For the hydrogen storage system, six Type II horizontal vessels, in steel, have been chosen, coming from a previous analysis [61,63]. Parameters for each tank are listed in Table 3.

Table 3 - Hydrogen Infrastructure Simulation Parameters

Component	Parameters	Value
Electrolyzer	Number of series-connected cells, $N_{el,cell}$ [-]	1800
	Membrane Cross Section Area, A_{el} [cm^2]	100
	Nominal Temperature [K]	353
	Nominal Pressure [bar]	10
	Operating Current [A]	135
	Electrolyzer Initial Temperature [K]	293
	Thermal Resistance, $R_{el,t}$ [°C/W]	0.09
	Specific Thermal Capacity $C_{el,t}$ [kJ/°C kW]	3
	Stand-by Power Consumption, $\%_{nom}$ [%]	10
Compressor	Compressor Flow Rate Parameter, $k_{c,1}$ [Nm^3/hr]	3.48
	Compressor Flow Rate Parameter, $k_{c,2}$ [Nm^3/hr Pa]	11.6
	Compressor Efficiency, η_m [-]	0.8
	Polytropic Coefficient, m [-]	1.609
	Suction Pressure [bar]	10
	Intercooler CoP [-]	1.5
	Maximum Pressure [bar]	350
Storage	Number of Tanks [-]	6
	Volume [m^3]	1.44
	Nominal Pressure [bar]	350
	Maximum Pressure [bar]	400
	Minimum Pressure [bar]	87.5
	Nominal Capacity [kg]	43.5

The trip and dispensing scheduling have been matched, as shown in Figure 4. The fueling ramp rate is considered 2.4 kg/min, intermediate among the common ramp rates (1.2 and 3.6 kg/min) [91]. The fueling time for the passenger train is 13 minutes and about 22 minutes for the freight transportation train. Since the route time for one trip is considered to be roughly 2 hours for the passenger trains, the refueling processes have been scheduled at 7 am, 10 am, 1 pm, 4 pm, and 7 pm. For freight transportation, the trains are considered in standby operation (SB) to be refueled at 9 am and 2 pm.

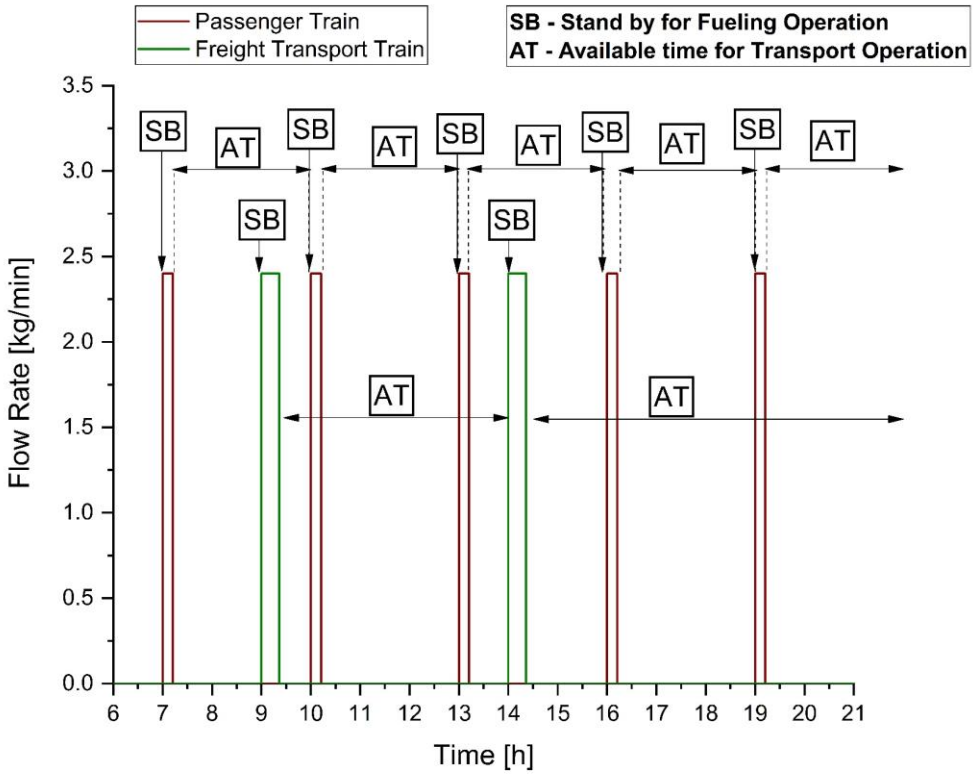
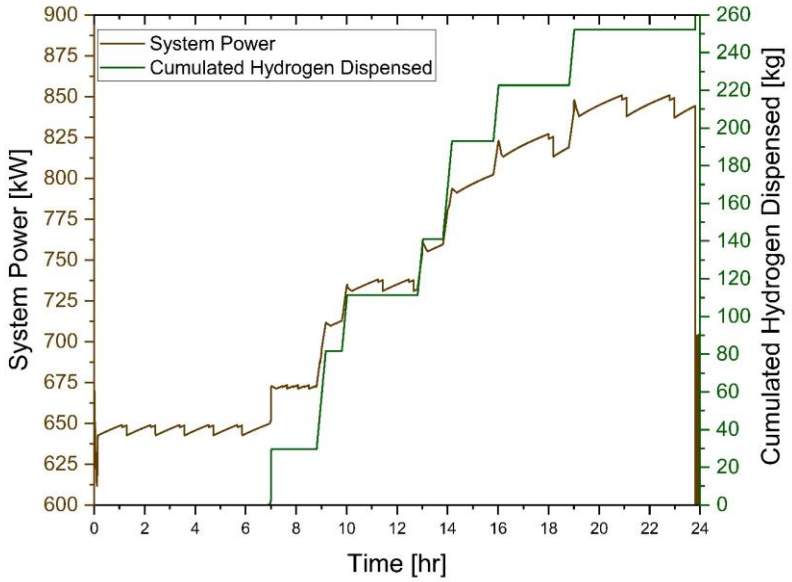
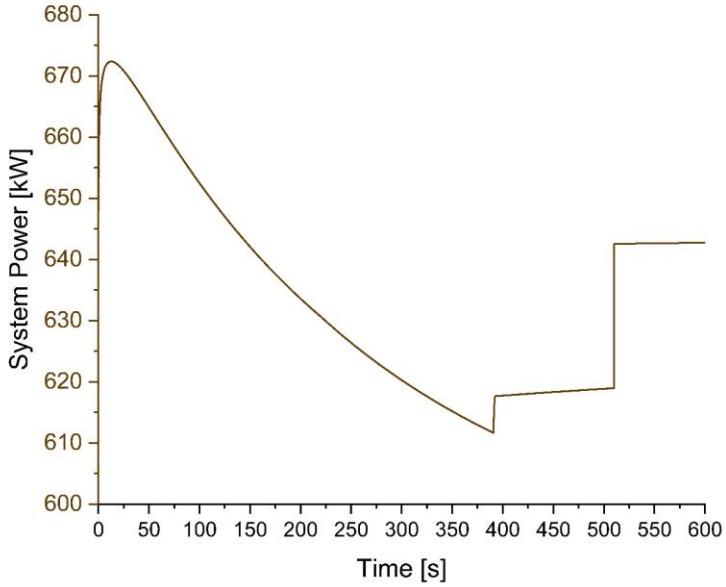


Figure 4 – Hydrogen Dispensing Scheduling

According to the dispensing schedule, the hydrogen station power trend is presented in Figure 5. The main power demanding component is the electrolyzer, with power consumption ranging from 670 kW during the startup phase, as shown in Figure 5b, stabilizing at 620 kW once the production is settled. The electrolyzer transient phase is conditioned by the thermal and pressure transients. The thermal transient is mainly referring to the electrolyzer target temperature achievement, set to 80°C. The initial electrolyzer temperature has been considered 20°C and processed as model input, with an external temperature of 20°C. When the electrolysis reaction occurs, heat is released according to the thermodynamic model explained in the "Numerical Modeling" Section. The cooling system provides the disposing of the excess heat generation, after the electrolysis having reached the chosen working parameters. Pressure transients occur at the very beginning of the electrolyzer operation when anodic and cathodic chambers are pressurized until the working pressure achieves the nominal operation target. Once the pressure target is met, the hydrogen storage compressor starts its operation. In Figure 5a it is possible to track the increase of the power trend when the refueling processes start. The storage is considered to be composed of two banks. Each bank has three hydrogen tanks. The main criteria and logic are to draw from the tank with the highest pressure level. Particularly, the first refueling processes require less energy, since the hydrogen within the storage tanks present high-pressure levels, as shown in Figure 6a and Figure 6b. When the hydrogen trains are refueled, the hydrogen pressure within the tank drops to lower levels. For this reason, the compressor power demand is higher for the latest refueling processes.

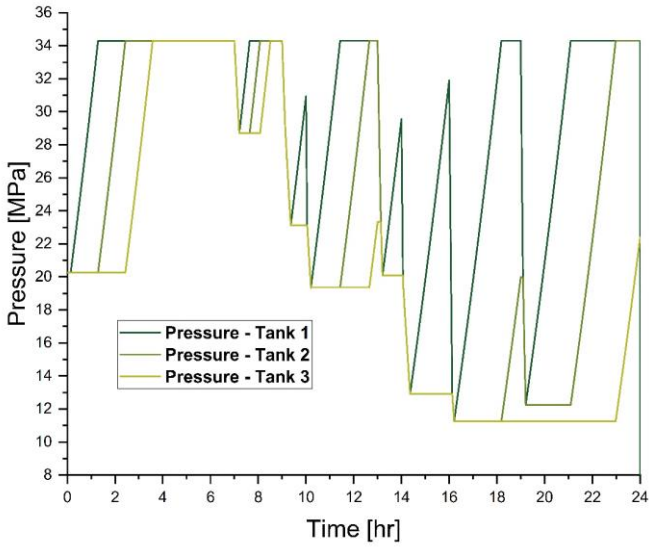


a)

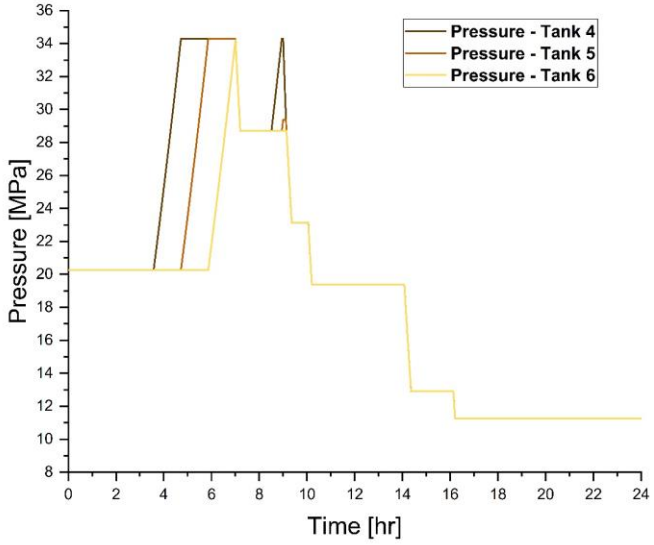


b)

Figure 5 – 260 kg/day Hydrogen Station, Power Demand and Hydrogen Dispensing for a daily operation (a) and Power Peak during the Start Up (b)



a)



b)

Figure 6 – Hydrogen Station, Storage Pressure Levels for Bank 1 (a) and Bank 2 (b), considering a production of 252 kg/day

The station sizing and daily performance have been analyzed for the most demanding scenario, with a daily hydrogen request for the trains of 252 kg. As for the train operation, a sensitive study is carried out, ranging from ±20% the trip passenger number and freight capacity. Figure 7 shows the results of this analysis. Considering 240 tons of goods and 120 passengers, the daily hydrogen station energy demand resulted to be 15.6 MWh/day, with a specific energy consumption of 61.8 kWh/kg of dispensed hydrogen and an LHV efficiency of 54%. The main energy rate belongs to the electrolyzer system, with a value of 57.2 kWh/kg, followed by the compressor, with a value of 3 kWh/kg, and by the dispensing process, 1.6 kWh/kg. As long as the hydrogen demand decreases, the electrolyzer, sized for the maximum capacity (260 kg), presents fewer working hours, and more hours when the unit is set in-standby mode, requiring 10% of its nominal power. The stand-by hours achieved in the lowest demanding scenario (160 tons of goods and 80 passengers) are slightly more than 1 hour, with a hydrogen dispensing demand of 243.5 kg/day. In

this case, the hydrogen station energy demand drops to 15.1 MWh/kg, with a specific power consumption of 62.1 kWh/kg of hydrogen dispensed and a system efficiency of 53.7%. The drops in the hydrogen demand do not heavily affect the specific energy consumption and the system efficiency, but the station results to require 500 kWh less in the lowest demanding case than the operation at full capacity.

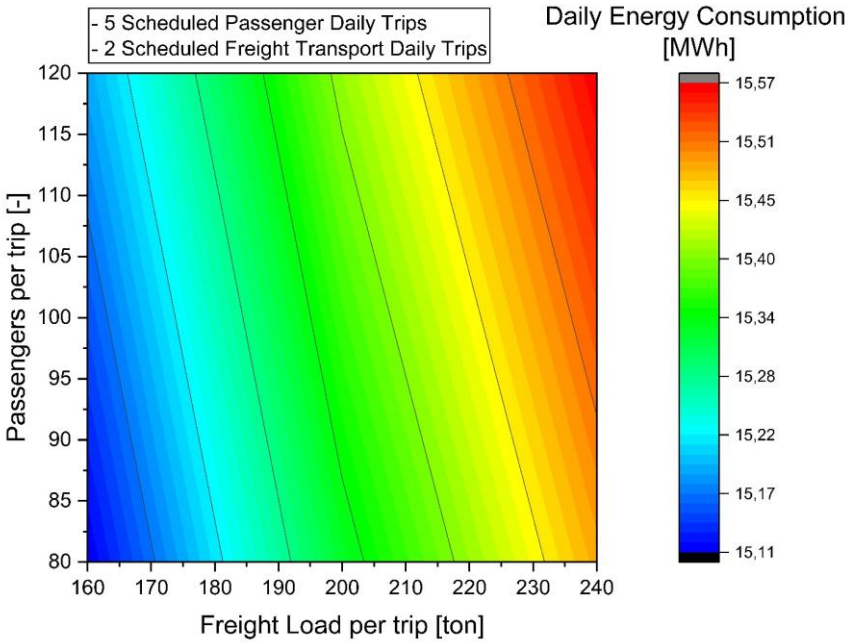


Figure 7 – Hydrogen Station Energy Demand under Different Transportation Scenarios

The energy performances of the investigated energy system have been then used as input parameters for the economic analysis. Considering the operation of the most demanding scenario (260 kg/day of hydrogen production and 252 kg/day of hydrogen dispensed), an economic assessment has been carried out. For the purposes of this analysis, the discount rate, *i*, has been set equal to 7%, according to the Italian Market, while the system lifespan set to 15 years, equal to the lifetime of the hydrogen trains. The general inflation rate, *g*, is considered to be equal to 3%, and the energy system availability is set to 95% of the annual potential railway sector working days (365 days/year).

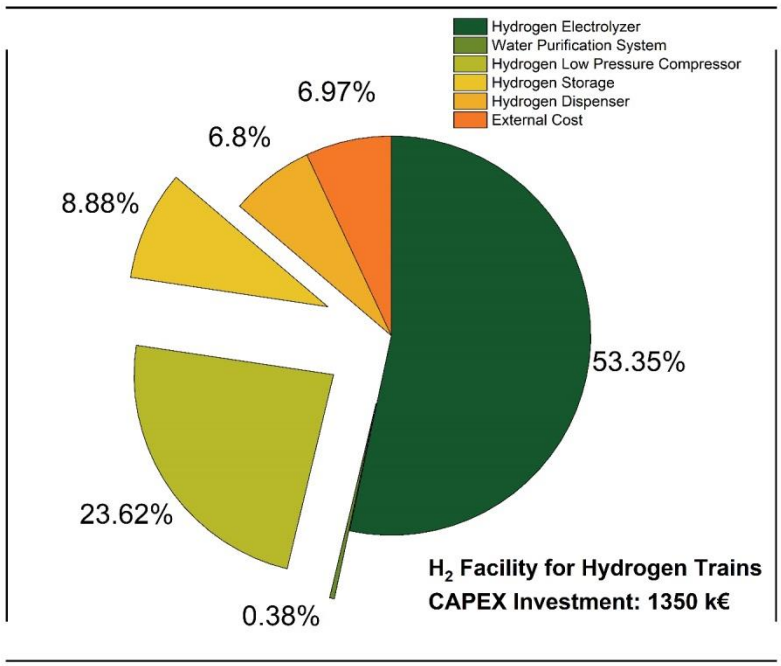
As the first step, the LCOH method has been applied, showing a value of 8.1 €/kg considering the on-site electrolytic production. With reference to the current Hydrogen Market [92,93], the hydrogen price has been considered to be 12 €/kg of hydrogen dispensed, with a profitable margin of almost 4 €/kg.

Once the hydrogen price has been set, the TCO of the whole system has been calculated, resulting in an overall value of 12.1 €/km, whose single-rate breakdown is composed of as follows: 3.23 €/km for the hydrogen train investments, 0.43 €/km for the hydrogen station facility investment, 2.22 €/km for the depreciation, 3.12 €/km for the fuel cost, 0.38 €/km for the labor cost, and 2.64 €/km for the maintenance activities.

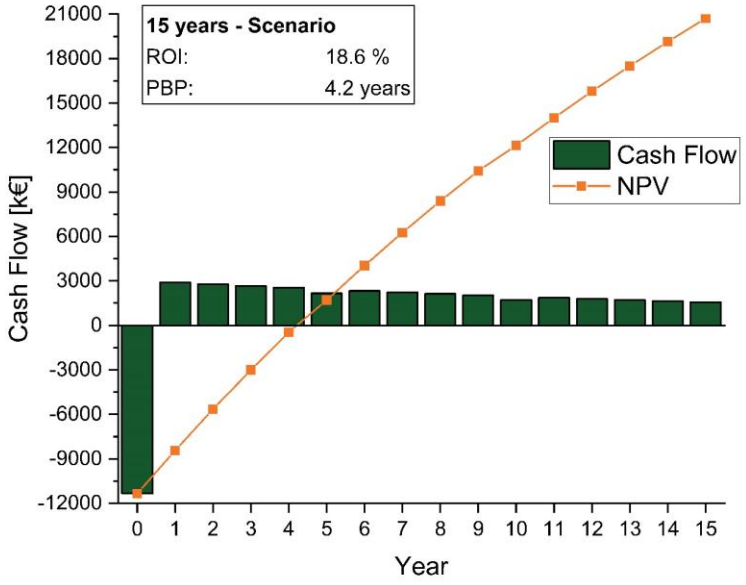
The calculated TCO shows a good match with European Union Hydrogen Train analysis [94], whose feasibility study for hydrogen trains reports a TCO value of 12 €/km under similar circumstances. In comparison with conventional technologies for a similar scenario [95], the investigated system resulted to have a TCO very close to the Diesel Train (8.8 €/km), and it represents a better option if compared to the full-battery electric train (14.8 €/km) and potential new electrification of the catenary (44.9 €/km) [95].

After the economic static analysis, a dynamic financial analysis has been carried out, considering a passenger ticket reference price of 5 €/trip according to the timetable and prices of regular trains belonging to the primary train operator in Italy [96], and a freight transport payload of 13 €/ton, according to current market tariffs for Southern Italy Regional Transport, retrieved from the Italian Company "TRT Trasporti e Territorio" 2018 report [97]. The main results are summarized in Figure 8. The initial investment accounts for almost 11350 k€, whose main rate belongs to the two hydrogen trains, with a specific investment of 5,000 k€ for each train. The hydrogen station cost breakdown is shown

in Figure 8a: the electrolyzer presents the main cost, with about 54 % of the facility cost, followed by the compressor (24%) and by the storage tanks (9%).
The discounted annual cash flows are shown in Figure 8b: at years 5 and 10, the annual cash flows present lower values due to electrolyzer stack replacements. The breakeven point is reached after a payback period of 4.2 years. Indeed, the business case has shown an overall NPV, at the end of the 15 years, of 20,000 k€, and an ROI of about 19%.



a)



b)

Figure 8 – Business Case Analysis: Hydrogen Facility Cost Breakdown (a) and Annual Cash Flow for the Hydrogen Train Station Facility (b)

4. CONCLUSIONS

Advanced and alternative technologies are worldwide investigated by industry and scientific community, proposing cleaner and more efficient solutions to the mobility sector, to replace the fossil fuel-based conventional vehicles. Hydrogen is already recognized as the most comprehensive energy vector, offering deep decarbonization and high energy performance when coupled with fuel cell technology.

In this train of thought, this article aimed to investigate the feasibility and the integration of a hydrogen refueling station for fuel cell hybrid trains, for passenger and freight transport. The analysis adopted the models implemented and presented by the authors, based on a dynamic and multi-physics approach, and applied to a Regional Scenario case study, in Southern Italy, with a track length of about 140 m, under the Water and Energy Italian Market assumptions.

An ad-hoc designed dispensing schedule has been considered, integrating the features and the operation of the hydrogen station with the fuel cell hybrid train performance and with the route features.

The powertrain components of the fuel cell hybrid trains have been sized and chosen: two 180 kW fuel cell stacks, and LFP battery packs, with two different configurations depending on the train type, if for passengers or freight.

The fuel cell system chosen for the passenger trains resulted to require about 29 kg/cycle of hydrogen, operating with an average efficiency of 50%, while for the freight transport the fuel cell stacks required about 52 kg/cycle of hydrogen, with an average efficiency of 47%.

To size the hydrogen fueling station, 1-day operations are considered. For passengers, 5 daily trips are scheduled, while 2 complete journeys are taken into account for goods transportation. Thanks to energy investigations on the hybrid train performance, according to the passenger and freight weight esteemed, about 250 kg of hydrogen per day are needed. The station resulted to be mainly composed of a 670 kW-PEM electrolyzer, operating at 10 bar with a working temperature of 80 °C, producing 260 kg of daily hydrogen, stored at 350 bar via a volumetric compressor, and dispensing 252 kg per day. The main energy share in the hydrogen station operation belongs to the PEM electrolyzer, whose power reached a maximum value of 670 kW during the startup phase, lowering to 620 kW once the electrolyzer operation stabilized. The station daily energy consumption has been evaluated, too, achieving approximately 15.6 MWh.

Considering the sized hydrogen station and the train operation, a sensitivity analysis is proposed, focusing on the main system parameters, ranging the passenger number and freight weight of ±20%. The passenger and freight trains required a total amount of 243.5 kg of hydrogen during a daily operation for 80 passengers and 160 tons of goods, and 252 kg of hydrogen for 120 passengers and 240 tons of goods. As main conclusions, the passenger rate variation presented a lower increase compared to the freight influence, given the related amount of mass.

Promising results are reached, demonstrating the feasibility and benefits of the system, also in terms of energy performance, with a facility energy efficiency over 50%, maintaining high values even in the most demanding scenarios. The drops in the hydrogen demand did not heavily affect the specific energy consumption and the system efficiency of the hydrogen station, but the station resulted to require 500 kWh less in the lowest demanding case than the operation at full capacity.

A sensitive analysis has been carried out considering suitable variations of passenger and freight transported and investigating the behavior of the fuel cell hybrid powertrain, whose operation in two trains reaches a maximum hydrogen consumption of 252 kg per day. According to the train consumption, a hydrogen facility has been conveniently sized and the daily energy consumption evaluated, achieving approximately 15.6 MWh.

In the last step, the economic investment needed for the integrated hydrogen system railway-infrastructure has been deeply investigated, using static and dynamic analyses, showing a levelized cost of hydrogen and a total cost of ownership respectively of about 8 €/kg and 12 €/km, a return on the investment of almost 19% and a payback period of 4.2 years.

The investigated case study showed how these technologies can provide a sustainable and valid option to the mobility sector, both from a technical point of view, by guaranteeing important values of infrastructure energy efficiency and a reduced train hydrogen consumption, and from an economic point of view, with acceptable return-on-investment and pay-back period. In particular, the achieved promising results confirm the huge potentiality of hydrogen use in heavy-duty transport applications, considering both the high performance and the positive economic

factors, and they highlight the feasibility of integrated systems fuel cell railway-hydrogen infrastructure for Regional scenarios.

ACKNOWLEDGMENTS
The research was supported by the grant PON RI 2014-2020 for Innovative Industrial PhD (CUP H25D18000120006 and Code DOT1305040), funded by the European Union and the Italian Ministry of Education, University and Research (MIUR).

AUTHORS CONTRIBUTION
All the authors equally contribute to the research activity, numerical simulations, and manuscript preparation.

DECLARATION OF INTERESTS
The authors declare that they have no known competing financial interests or personal relationships that could have appeared to influence the work reported in this paper.

NOMENCLATURE

$\%_{nom}$	Stand-by Power Consumption [%]
A_{el}	Active Electrolytic Cell Area [cm^2]
AP_{H_2}	Hydrogen Annual Production [kg]
b	Exponential Coefficient for Electrolyzer Ancillary Power Consumption, 0.249 [-]
c	Consumption [g s-1]
C_{capex}	Capital Expenditure Cost [€]
$C_{el,t}$	Total thermal capacity of the electrolyzer [kJ/K]
C_{fuel}	Fuel Cost [€]
C_{labor}	Labor Cost [€]
C_{opex}	Operational Expenditure Cost [€]
C_{rep}	Replacement Cost [€]
CF_x	Cash Flow per year [€]
CoP	Coefficient of Performance [-]
D	Depreciation [€]
E_0	No load voltage [V]
E_n	Nernst voltage [V]
E_{rev}	Reversible Voltage [V]
E_{tn}	Thermo-neutral Voltage [V]
F	Force
g	General inflation rate [-]
i	Discount rate [-]
I	Direct Current [A]
$I_{0,lim}$	Exchange current, 4.576e-05 [A]
$I_{el,lim}$	Limit current, 140.1 [A]
k_0	Faraday Efficiency Coefficient, -0.0922 [-]
k_1	Faraday Efficiency Coefficient, 0.0091 $\left[\frac{1}{A}\right]$
k_2	Faraday Efficiency Coefficient, 0.00003 $\left[\frac{1}{A^2}\right]$
k_3	Faraday Efficiency Coefficient, 0.0000003 $\left[\frac{1}{A^3}\right]$
k_{anc}	Coefficient for Electrolyzer Ancillary Power Consumption, 0.193 [W]
$k_{c,1}$	Compressor Flow Rate Parameter [Nm^3/hr]
$k_{c,2}$	Compressor Flow Rate Parameter [$Nm^3/(hr \cdot Pa)$]
$k_{Dav,1}$	First Davis Coefficient [N]
$k_{Dav,2}$	Second Davis Coefficient [N s m-1]
$k_{Dav,3}$	Third Davis Coefficient [N s2 m-2]
k_{ECMS}	Equivalence factor [-]
k_F	Faraday constant, 96485000 [Coulomb/kmol]
k_p	Polarization resistance [Ω]
LHV	Hydrogen lower heating value, 33.3 [kWh/kg]
m	Polytropic Coefficient [-]
$\dot{m}$	Mass Flow Rate [kg/s]
M	Mass [kg]
MW	Molecular Weight [kg/kmol]
n	Life span of the system [yr]
N_{cell}	Number of cells [-]
NPV	Net Present Value [€]
p	Pressure [Pa]
q	Number of Components needed replacement [-]
Q	Capacity [Ah]
Q_e	Exponential capacity [(Ah)-1]
$\dot{Q}_{cool}$	Heat transfer rate required to cool down the system [W]
r_j	Year of Replacement [yr]
R	Universal gas constant, 8314.3 [$J/(kmol \cdot K)$]
R_B	Battery internal resistance [Ω]
$R_{el,t}$	Total thermal resistance of the electrolyzer [K/W]
R_g	Hydrogen gas constant, 4124.2 [$J/(kg \cdot K)$]
RP	Reselling Price [€]
S	Capacity factor for low frequency currents [-]

t	Time [s]
t_m	Membrane Thickness, 0.03306 [cm]
T	Temperature [K]
TD	Train Total Distance per year [km]
U	Voltage [V]
v	Speed [m s-1]
W	Power [W]
$W_{el,nom}$	Electrolyzer Nominal Power [W]
$W_{el,stack}$	Electrolyzer Stack Actual Power [W]
z	Number of free electrons [-]

Greek

α	Charge transfer coefficient, 0.5316 [-]
β	Empirical Coefficient, 0.315 [-]
γ	Track slope angle [grad]
ΔG_0	Standard Gibbs energy [J mol-1]
η_m	Compressor Efficiency [-]
λ_m	Membrane Water Content, 17 [-]

Subscript

a	Parameter related to average ambient conditions
anc	Parameter related to the ancillary system
B	Parameter related to battery
c	Parameter related to the compressor
cell	Parameter related to the cell
e	Exponential value
eff	Effective value
el	Parameter related to electrolyzer
eq	Equivalent value
FC	Parameter related to fuel cell
H_2	Parameter related to hydrogen
H_2O	Parameter related to water
in	Parameter in input to the system
lf	Parameter related to low frequency dynamics
max	Maximum Value
nom	Parameter related to nominal condition
O_2	Parameter related to oxygen
out	Parameter in output from the system
p	Parameter related to the hydrogen production
res	Parameter related to resistance losses
tank	Parameter related to the tank
target	Value to achieve
tr	Parameter related to traction
T	Total value
v	Parameter related to the vehicle

Abbreviation

B	Battery
CAPEX	Capital Expenditures
CFR	Capital Recovery Factor
DC	Direct current
ECMS	Equivalent consumption minimization strategy
FC	Fuel cell
FCEV	Fuel Cell Electric Vehicle
LCOH	Levelized Cost of Hydrogen
LFP	Lithium iron phosphate
OPEX	Operational Expenditures
PEM	Polymer Electrolyte Membrane

ROI	Return on Investment
SOC	State of charge
TCO	Total Cost of Ownership

REFERENCES

[1] Kılkış Ş, Krajačić G, Duić N, Montorsi L, Wang Q, Rosen MA, et al. Research frontiers in sustainable development of energy, water and environment systems in a time of climate crisis. Energy Convers Manag 2019. https://doi.org/10.1016/j.enconman.2019.111938.

[2] Santika WG, Anisuzzaman M, Bahri PA, Shafiullah GM, Rupf G V., Urmee T. From goals to joules: A quantitative approach of interlinkages between energy and the Sustainable Development Goals. Energy Res Soc Sci 2019. https://doi.org/10.1016/j.erss.2018.11.016.

[3] Steffen B, Egli F, Pahle M, Schmidt TS. Navigating the Clean Energy Transition in the COVID-19 Crisis. Joule 2020. https://doi.org/10.1016/j.joule.2020.04.011.

[4] You C, Kim J. Optimal design and global sensitivity analysis of a 100% renewable energy sources based smart energy network for electrified and hydrogen cities. Energy Convers Manag 2020;223:113252. https://doi.org/https://doi.org/10.1016/j.enconman.2020.113252.

[5] The Future of Hydrogen. 2019. https://doi.org/10.1787/1e0514c4-en.

[6] Abdin Z, Mérida W. Hybrid energy systems for off-grid power supply and hydrogen production based on renewable energy: A techno-economic analysis. Energy Convers Manag 2019. https://doi.org/10.1016/j.enconman.2019.06.068.

[7] Abdalla AM, Hossain S, Nisfindy OB, Azad AT, Dawood M, Azad AK. Hydrogen production, storage, transportation and key challenges with applications: A review. Energy Convers Manag 2018. https://doi.org/10.1016/j.enconman.2018.03.088.

[8] Apostolou D, Xydis G. A literature review on hydrogen refuelling stations and infrastructure. Current status and future prospects. Renew Sustain Energy Rev 2019. https://doi.org/10.1016/j.rser.2019.109292.

[9] Matute G, Yusta JM, Correas LC. Techno-economic modelling of water electrolysers in the range of several MW to provide grid services while generating hydrogen for different applications: A case study in Spain applied to mobility with FCEVs. Int J Hydrogen Energy 2019. https://doi.org/10.1016/j.ijhydene.2019.05.092.

[10] Mayyas A, Mann M. Manufacturing competitiveness analysis for hydrogen refueling stations. Int J Hydrogen Energy 2019. https://doi.org/10.1016/j.ijhydene.2019.02.135.

[11] Sdanghi G, Maranzana G, Celzard A, Fierro V. Review of the current technologies and performances of hydrogen compression for stationary and automotive applications. Renew Sustain Energy Rev 2019. https://doi.org/10.1016/j.rser.2018.11.028.

[12] Ligen Y, Vrubel H, Arlettaz J, Girault H. Experimental correlations and integration of gas boosters in a hydrogen refueling station. Int J Hydrogen Energy 2020. https://doi.org/10.1016/j.ijhydene.2020.04.162.

[13] Genovese M, Blekhman D, Xie C, Dray M, Fragiacomo P. Assuring pulsation-free flow in a directly pressurized fuel delivery at a retail hydrogen station. Int J Hydrogen Energy 2018;43:16623–37. https://doi.org/10.1016/j.ijhydene.2018.07.024.

[14] Kurtz J, Sprik S, Bradley TH. Review of transportation hydrogen infrastructure performance and reliability. Int J Hydrogen Energy 2019. https://doi.org/10.1016/j.ijhydene.2019.03.027.

[15] Qian J, Li X, Gao Z, Jin Z. A numerical study of unintended hydrogen release in a hydrogen refueling station. Int J Hydrogen Energy 2020;45:20142–52. https://doi.org/https://doi.org/10.1016/j.ijhydene.2020.05.063.

[16] Hansen OR. Hydrogen infrastructure—Efficient risk assessment and design optimization approach to ensure safe and practical solutions. Process Saf Environ Prot 2020. https://doi.org/10.1016/j.psep.2020.06.028.

[17] Piera M, Martínez-Val JM, José Montes M. Safety issues of nuclear production of hydrogen. Energy Convers Manag 2006. https://doi.org/10.1016/j.enconman.2006.02.002.

[18] Ustolin F, Paltrinieri N, Berto F. Loss of integrity of hydrogen technologies: A critical review. Int J Hydrogen Energy 2020. https://doi.org/https://doi.org/10.1016/j.ijhydene.2020.06.021.

[19] Kurtz J, Sprik S, Peters M, Bradley TH. Retail Hydrogen Station Reliability Status and Advances. Reliab Eng Syst Saf 2020. https://doi.org/10.1016/j.ress.2020.106823.

[20] Sørensen B, Spazzafumo G. Implementation scenarios. Hydrog. Fuel Cells, 2018. https://doi.org/10.1016/b978-0-08-100708-2.00005-9.

[21] Frischauf N. Hydrogen-fueled spacecraft and other space applications of hydrogen. Compend. Hydrog. Energy, 2016. https://doi.org/10.1016/b978-1-78242-364-5.00005-1.

[22] Gye HR, Seo SK, Bach QV, Ha D, Lee CJ. Quantitative risk assessment of an urban hydrogen

refueling station. Int J Hydrogen Energy 2019. https://doi.org/10.1016/j.ijhydene.2018.11.035.

[23] Hydrogen Tool Portal 2019. https://h2tools.org/lessons (accessed October 26, 2019).

[24] Gu Y, Chen Q, Xue J, Tang Z, Sun Y, Wu Q. Comparative techno-economic study of solar energy integrated hydrogen supply pathways for hydrogen refueling stations in China. Energy Convers Manag 2020;223:113240. https://doi.org/https://doi.org/10.1016/j.enconman.2020.113240.

[25] Kiaee M, Cruden A, Chladek P, Infield D. Demonstration of the operation and performance of a pressurised alkaline electrolyser operating in the hydrogen fuelling station in Porsgrunn, Norway. Energy Convers Manag 2015. https://doi.org/10.1016/j.enconman.2015.01.070.

[26] Lee B, Heo J, Kim S, Sung C, Moon C, Moon S, et al. Economic feasibility studies of high pressure PEM water electrolysis for distributed H2 refueling stations. Energy Convers Manag 2018. https://doi.org/10.1016/j.enconman.2018.02.041.

[27] Ismail TM, Ramzy K, Elnaghi BE, Abelwhab MN, El-Salam MA. Using MATLAB to model and simulate a photovoltaic system to produce hydrogen. Energy Convers Manag 2019;185:101–29. https://doi.org/10.1016/j.enconman.2019.01.108.

[28] Groppi D, Astiaso Garcia D, Lo Basso G, Cumo F, De Santoli L. Analysing economic and environmental sustainability related to the use of battery and hydrogen energy storages for increasing the energy independence of small islands. Energy Convers Manag 2018. https://doi.org/10.1016/j.enconman.2018.09.063.

[29] Mehrjerdi H, Iqbal A, Rakhshani E, Torres JR. Daily-seasonal operation in net-zero energy building powered by hybrid renewable energies and hydrogen storage systems. Energy Convers Manag 2019. https://doi.org/10.1016/j.enconman.2019.112156.

[30] Xu C, Ke Y, Li Y, Chu H, Wu Y. Data-driven configuration optimization of an off-grid wind/PV/hydrogen system based on modified NSGA-II and CRITIC-TOPSIS. Energy Convers Manag 2020. https://doi.org/10.1016/j.enconman.2020.112892.

[31] Bhattacharyya R, Misra A, Sandeep KC. Photovoltaic solar energy conversion for hydrogen production by alkaline water electrolysis: Conceptual design and analysis. Energy Convers Manag 2017. https://doi.org/10.1016/j.enconman.2016.11.057.

[32] Fragiacomo P, Genovese M. Technical-economic analysis of a hydrogen production facility for power-to-gas and hydrogen mobility under different renewable sources in Southern Italy. Energy Convers Manag 2020;223:113332. https://doi.org/https://doi.org/10.1016/j.enconman.2020.113332.

[33] Bögel P, Oltra C, Sala R, Lores M, Upham P, Dütschke E, et al. The role of attitudes in technology acceptance management: Reflections on the case of hydrogen fuel cells in Europe. J Clean Prod 2018. https://doi.org/10.1016/j.jclepro.2018.03.266.

[34] Wang Y, Ruiz Diaz DF, Chen KS, Wang Z, Adroher XC. Materials, technological status, and fundamentals of PEM fuel cells – A review. Mater Today 2020. https://doi.org/10.1016/j.mattod.2019.06.005.

[35] Desantes JM, Molina S, Novella R, Lopez-Juarez M. Comparative global warming impact and NOX emissions of conventional and hydrogen automotive propulsion systems. Energy Convers Manag 2020. https://doi.org/10.1016/j.enconman.2020.113137.

[36] Balali Y, Stegen S. Review of energy storage systems for vehicles based on technology, environmental impacts, and costs. Renew Sustain Energy Rev 2021;135:110185. https://doi.org/https://doi.org/10.1016/j.rser.2020.110185.

[37] Garmsiri S, Dincer I, Naterer GF. Comparisons of automotive, locomotive, aircraft and marine conversion to hydrogen propulsion using six-sigma methodologies. Int J Hydrogen Energy 2013. https://doi.org/10.1016/j.ijhydene.2012.11.088.

[38] Hoffrichter A, Hillmansen S, Roberts C. Conceptual propulsion system design for a hydrogen-powered regional train. IET Electr Syst Transp 2016. https://doi.org/10.1049/iet-est.2014.0049.

[39] Furuya T, Ogawa K, Yamamoto T. Drive control for fuel cells and lithium ion battery hybrid railway vehicle. 5th IEEE Veh. Power Propuls. Conf. VPPC '09, 2009. https://doi.org/10.1109/VPPC.2009.5289867.

[40] Siddiqui O, Dincer I. A Review on Fuel Cell-Based Locomotive Powering Options for Sustainable Transportation. Arab J Sci Eng 2019. https://doi.org/10.1007/s13369-018-3607-2.

[41] Fragiacomo P, Piraino F. Fuel Cell-Based Powertrain Analysis for Tramway Systems. SAE Tech. Pap., 2019. https://doi.org/10.4271/2019-24-0248.

[42] Fernandez LM, Garcia P, Garcia CA, Torreglosa JP, Jurado F. Comparison of control schemes for a fuel cell hybrid tramway integrating two dc/dc converters. Int J Hydrogen Energy 2010. https://doi.org/10.1016/j.ijhydene.2010.02.132.

[43] Fernandez LM, Garcia P, Garcia CA, Jurado F. Hybrid electric system based on fuel cell and battery

and integrating a single dc/dc converter for a tramway. Energy Convers Manag 2011. https://doi.org/10.1016/j.enconman.2010.12.028.

[44] Zhang W, Li J, Xu L, Ouyang M. Optimization for a fuel cell/battery/capacity tram with equivalent consumption minimization strategy. Energy Convers Manag 2017. https://doi.org/10.1016/j.enconman.2016.11.007.

[45] Zhang H, Yang J, Zhang J, Song P, Xu X. A firefly algorithm optimization-based equivalent consumption minimization strategy for fuel cell hybrid light rail vehicle. Energies 2019. https://doi.org/10.3390/en12142665.

[46] Piraino F, Fragiacomo P. A multi-method control strategy for numerically testing a fuel cell-battery-supercapacitor tramway. Energy Convers Manag 2020;225:113481. https://doi.org/https://doi.org/10.1016/j.enconman.2020.113481.

[47] Miller AR, Hess KS, Barnes DL, Erickson TL. System design of a large fuel cell hybrid locomotive. J Power Sources 2007. https://doi.org/10.1016/j.jpowsour.2007.08.045.

[48] Peng F, Chen W, Liu Z, Li Q, Dai C. System integration of China's first proton exchange membrane fuel cell locomotive. Int. J. Hydrogen Energy, 2014. https://doi.org/10.1016/j.ijhydene.2014.01.166.

[49] Reddi K, Elgowainy A, Rustagi N, Gupta E. Impact of hydrogen refueling configurations and market parameters on the refueling cost of hydrogen. Int J Hydrogen Energy 2017;42:21855–65. https://doi.org/10.1016/j.ijhydene.2017.05.122.

[50] Fragiacomo P, Piraino F, Genovese M. Insights for Industry 4 . 0 Applications into a Hydrogen Advanced Mobility. Procedia Manuf 2020;42:239–45. https://doi.org/10.1016/j.promfg.2020.02.077.

[51] Fragiacomo P, Piraino F. Fuel cell hybrid powertrains for use in Southern Italian railways. Int J Hydrogen Energy 2019. https://doi.org/10.1016/j.ijhydene.2019.09.005.

[52] Fragiacomo P, Piraino F. Numerical modelling of a PEFC powertrain system controlled by a hybrid strategy for rail urban transport. J Energy Storage 2018;17:474–84. https://doi.org/10.1016/j.est.2018.04.011.

[53] Tremblay O. Experimental Validation of a Battery Dynamic Model for EV Applications Experimental Validation of a Battery Dynamic Model for EV Applications. 24th Int Batter Hybrid Fuel Cell Electr Veh Symp Exhib 2009, EVS 24 2015.

[54] Espinosa-López M, Darras C, Poggi P, Glises R, Baucour P, Rakotondrainibe A, et al. Modelling and experimental validation of a 46 kW PEM high pressure water electrolyzer. Renew Energy 2018;119:160–73. https://doi.org/10.1016/j.renene.2017.11.081.

[55] Abdol Rahim AH, Tijani AS, Kamarudin SK, Hanapi S. An overview of polymer electrolyte membrane electrolyzer for hydrogen production: Modeling and mass transport. J Power Sources 2016;309:56–65. https://doi.org/10.1016/j.jpowsour.2016.01.012.

[56] Olivier P, Bourasseau C, Bouamama PB. Low-temperature electrolysis system modelling: A review. Renew Sustain Energy Rev 2017;78:280–300. https://doi.org/10.1016/j.rser.2017.03.099.

[57] Fragiacomo P, Genovese M. Modeling and energy demand analysis of a scalable green hydrogen production system. Int J Hydrogen Energy 2019;44:30237–55. https://doi.org/10.1016/j.ijhydene.2019.09.186.

[58] Ulleberg Ø. Modeling of advanced alkaline electrolyzers: A system simulation approach. Int J Hydrogen Energy 2003. https://doi.org/10.1016/S0360-3199(02)00033-2.

[59] Zheng J, Ye J, Yang J, Tang P, Zhao L, Kern M. An optimized control method for a high utilization ratio and fast filling speed in hydrogen refueling stations. Int J Hydrogen Energy 2010;35:3011–7. https://doi.org/10.1016/j.ijhydene.2009.07.001.

[60] Rothuizen ED. Hydrogen Fuelling Stations A Thermodynamic Analysis of Fuelling Hydrogen Vehicles for Personal Transportation. Technical University of Denmark, 2013.

[61] Fragiacomo P, Genovese M. Numerical simulations of the energy performance of a PEM water electrolysis based high-pressure hydrogen refueling station. Int J Hydrogen Energy 2020;45:27457–70. https://doi.org/10.1016/j.ijhydene.2020.07.007.

[62] Reddi K, Elgowainy A, Rustagi N, Gupta E. Two-tier pressure consolidation operation method for hydrogen refueling station cost reduction. Int J Hydrogen Energy 2018;43:2919–29. https://doi.org/10.1016/j.ijhydene.2017.12.125.

[63] Fragiacomo P, Genovese M. Developing a Mathematical Tool for Hydrogen Production, Compression and Storage. Int J Hydrogen Energy 2020. https://doi.org/10.1016/j.ijhydene.2020.04.269.

[64] Sunita Satyapal, Director H and FCP. FY 2018 PROGRESS REPORT FOR THE DOE HYDROGEN AND FUEL CELLS PROGRAM. 2019.

[65] Reuß M, Grube T, Robinius M, Preuster P, Wasserscheid P, Stolten D. Seasonal storage and

alternative carriers: A flexible hydrogen supply chain model. Appl Energy 2017;200:290–302. https://doi.org/10.1016/j.apenergy.2017.05.050.

[66] Othman E-SA, Nawar SK, Fahmy FH, El-Shafy A, Nafeh A. A New design of A Hydrogen Fueling Station Powered By Renewable Energy Sources. IOSR J Electr Electron Eng Ver II 2015;10:2278–1676. https://doi.org/10.9790/1676-1052116125.

[67] Mayer T, Semmel M, Guerrero Morales MA, Schmidt KM, Bauer A, Wind J. Techno-economic evaluation of hydrogen refueling stations with liquid or gaseous stored hydrogen. Int J Hydrogen Energy 2019. https://doi.org/10.1016/j.ijhydene.2019.08.051.

[68] Elgowainy A. Techno-economic Tools to Simulate the Costs of Hydrogen Infrastructure Technologies. 2018.

[69] Tractebel E, Engie, Hinicio. Study on Early Business Cases for H2 in Energy Storage and More Broadly Power To H2 Applications. EU Comm 2017:228.

[70] Oldenbroek V, Verhoef LA, van Wijk AJM. Fuel cell electric vehicle as a power plant: Fully renewable integrated transport and energy system design and analysis for smart city areas. Int J Hydrogen Energy 2017. https://doi.org/10.1016/j.ijhydene.2017.01.155.

[71] FCH; Roland Berger; Development of Business Cases for Fuel Cells and Hydrogen Applications for Regions and Cities. Consol Technol Introd Dossiers Brussels FCH JU 2017:18.

[72] Acque N. Water Tariffs n.d. http://www.nuoveacque.it/tariffe/202/140/1/#industrialegrandiquantitativi (accessed March 3, 2020).

[73] Bertolini M, D'Alpaos C, Moretto M. Electricity prices in Italy: Data registered during photovoltaic activity interval. Data Br 2018. https://doi.org/10.1016/j.dib.2018.06.018.

[74] GME. GME - Gestore Mercati Energetici, Italy 2020. https://www.mercatoelettrico.org/It/Tools/Accessodati.aspx?ReturnUrl=%2Fit%2FStatistiche%2FME%2FPrezzoMedioFasce.aspx (accessed April 27, 2020).

[75] ARERA. Autorità di Regolazione per Energia Reti e Ambiente (ARERA) n.d. http://www.autorita.energia.it/it/dati/eep38.htm (accessed April 27, 2020).

[76] Viktorsson L, Heinonen JT, Skulason JB, Unnthorsson R. A step towards the hydrogen economy - A life cycle cost analysis of a hydrogen refueling station. Energies 2017. https://doi.org/10.3390/en10060763.

[77] Moon S, Lee DJ. An optimal electric vehicle investment model for consumers using total cost of ownership: A real option approach. Appl Energy 2019. https://doi.org/10.1016/j.apenergy.2019.113494.

[78] Jones J, Genovese A, Tob-Ogu A. Hydrogen vehicles in urban logistics: A total cost of ownership analysis and some policy implications. Renew Sustain Energy Rev 2020. https://doi.org/10.1016/j.rser.2019.109595.

[79] Lega Ambiente. Rapporto Pendolaria 2018. 2018.

[80] Piraino F, Fragiacomo P. Design of an Equivalent Consumption Minimization Strategy-Based Control in Relation to the Passenger Number for a Fuel Cell Tram Propulsion. Energies 2020;13:4010. https://doi.org/10.3390/en13154010.

[81] Genovese M, Blekhman D, Dray M, Fragiacomo P. Hydrogen losses in fueling station operation. J Clean Prod 2020;248:119266. https://doi.org/10.1016/j.jclepro.2019.119266.

[82] Lebbal ME, Lecœuche S. Identification and monitoring of a PEM electrolyser based on dynamical modelling. Int J Hydrogen Energy 2009;34:5992–9. https://doi.org/10.1016/j.ijhydene.2009.02.003.

[83] Ulleberg Ø. Stand-alone power systems for the future: optimal design, operation and control of solar-hydrogen energy systems. Norwegian University of Science and Technology, Trondheim [PhD dissertation], 1999.

[84] Diéguez PM, Ursúa A, Sanchis P, Sopena C, Guelbenzu E, Gandía LM. Thermal performance of a commercial alkaline water electrolyzer: Experimental study and mathematical modeling. Int J Hydrogen Energy 2008;33:7338–54. https://doi.org/10.1016/j.ijhydene.2008.09.051.

[85] Jannelli E, Minutillo M, Perna A. Analyzing microcogeneration systems based on LT-PEMFC and HT-PEMFC by energy balances. Appl Energy 2013;108:82–91. https://doi.org/10.1016/j.apenergy.2013.02.067.

[86] Valverde-Isorna L, Ali D, Hogg D, Abdel-Wahab M. Modelling the performance of wind-hydrogen energy systems: Case study the Hydrogen Office in Scotland/UK. Renew Sustain Energy Rev 2016;53:1313–32. https://doi.org/10.1016/j.rser.2015.08.044.

[87] Musio F, Tacchi F, Omati L, Gallo Stampino P, Dotelli G, Limonta S, et al. PEMFC system simulation in MATLAB-Simulink®environment. Int J Hydrogen Energy 2011;36:8045–52. https://doi.org/10.1016/j.ijhydene.2011.01.093.

[88] Dursun E, Acarkan B, Kilic O. Modeling of hydrogen production with a stand-alone renewable hybrid power system. Int J Hydrogen Energy 2012. https://doi.org/10.1016/j.ijhydene.2011.11.029.

[89] Zhao L, Brouwer J. Dynamic operation and feasibility study of a self-sustainable hydrogen fueling station using renewable energy sources. Int J Hydrogen Energy 2015;40:3822–37. https://doi.org/10.1016/j.ijhydene.2015.01.044.

[90] Zhao L, Brouwer J, Samuelsen S. Dynamic Analysis of a Self-Sustainable Renewable Hydrogen Fueling Station. ASME 2014 12th Int Conf Fuel Cell Sci Eng Technol 2014:V001T02A001. https://doi.org/10.1115/FuelCell2014-6330.

[91] Elgowainy A, Reddi K. Heavy-Duty Fuel Cell Vehicle Fleet. 2017.

[92] California Energy Commission, California Air Resources Board. Joint Agency Staff Report on Assembly Bill 8: Assessment of Time and Cost Needed to Attain 100 Hydrogen Refueling Stations in California. 2019.

[93] Roland Berger, Fuel Cells and Hydrogen Joint Undertaking. Fuel Cells and Hydrogen for Green Energy in European Cities and Regions. A Study for the Fuel Cells and Hydrogen Joint Undertaking. 2018.

[94] Roland Berger, Shift2Rail Joint Undertaking and Fuel Cells and Hydrogen Joint Undertaking 2019. Study on the Use of Fuel Cells & Hydrogen in the Railway Environment - Final. 2019. https://doi.org/10.2881/487836.

[95] Roland Berger, Shift2Rail Joint Undertaking and Fuel Cells and Hydrogen Joint Undertaking 2019. Study on the Use of Fuel Cells & Hydrogen in the Railway Environment - Report 2. 2019.

[96] Trenitalia. Train Timetables and Connections 2020. https://www.trenitalia.com/it/informazioni/acquisti_online.html (accessed October 14, 2020).

[97] TRT Trasporti e Territorio, Pastori E, Brambilla M. Italian Report on Railway Transport. Sistema Ferroviario di Trasporto Merci Automatico – Analisi dei costi di trasporto. Milan: 2018.